Politecnico di Torino

Master's Degree in Biomedical Engineering

Master's Thesis

3D printing of molecularly imprinted polymers for biomolecule removal

Supervisor:
Dott. Ignazio Roppolo

Candidate:
Arianna Diano

A.Y. 2024/2025

Contents

Abstract

Molecularly imprinted polymers, or MIPs, are artificial receptors developed thanks to the molecular imprinting technology, which allows the formation of specific binding sites created in a polymeric matrix. Since the size, shape, and functional groups of these cavities complement a target molecule (template) with high selectivity and specificity, MIPs can be employed to mimic the molecular recognition capabilities of natural biological receptors.

The advantages of MIPs over natural receptors include superior mechanical strength, resistance to harsh environmental conditions (like high temperatures and pressures), lower production costs, simplicity of synthesis, and remarkable template selection versatility. A wide range of industries, including drug delivery, biosensing, separation science, purification, analytical assays, catalysis, and artificial antibodies, have become increasingly interested in MIPs due to these features.

Molecularly Imprinted Polymers (MIPs) can be classified into two main categories: hard and soft MIPs. Hard MIPs are characterized by high stability and high selectivity, although the removal of the template molecule is often complex due to the strong interactions involved. In contrast, soft MIPs exhibit moderate selectivity and lower stability, as they rely on reversible interactions, which also allow for easier template removal. The mechanical properties are determined by the characteristics of the monomers and the crosslinkers selected to create the polymeric network, together with an initiator that is needed to start the polymerization process. The last element necessary for the MIPs fabrication is obviously the template, i.e. the target molecule to be recognized.

In this context, in this Thesis two molecules were tested as template molecules: oxytetracycline (OTC), an antibiotic with pharmaceutical and environmental significance, and bovine serum albumin (BSA), a frequently used model protein.

Following previous studies, in this thesis Hard MIPs that used OTC as a template were fabricated employing Digital Light Processing (DLP), a high-resolution 3D printing method that makes possible to fabricate intricate, self-supporting polymeric structures. Then the efficacy of the MIPs was investigated to be able to capture the target molecule in a controlled environment, analyzing it using the UV-Vis. OTC-MIP produced in this way could be seen as an

alternative to treat antibiotic-contaminated water and could lead to the development of a more efficient and sustainable water purification system.

In parallel, preliminary studies were carried out on Soft MIPs where BSA was selected as template molecule. In this case a resin containing BSA was formulated and polymerized. This material was then characterized using UV-Vis spectroscopy, investigating MIP capability and the effect of the various ingredients on protein stability.

Summarizing, this study aims at studying hard and soft MIPs, trying to establish bottlenecks and capabilities of next/generation artificial receptors.

1.Molecularly Imprinted Polymers (MIPs): Principles, Components

In recent decades, the field of molecular recognition has witnessed significant advances, particularly with the development of synthetic materials capable of mimicking biological receptors. Specific molecular recognition is the essential process controlling both biological form and function. This biological phenomenon is mainly mediated by proteins, complex macromolecules with regions capable of interacting with and binding to target molecules in a highly regulated way. They have applicability across different fields, including the selective detection of protein targets, clinical diagnostics and recuperative monitoring, the detection of organisms and toxins, along with bioterror agents. [1]

Among these synthetic polymers, Molecularly Imprinted Polymers (MIPs) have emerged as a powerful class of materials designed to selectively recognize and bind specific target molecules. MIPs possess highly specific binding sites formed during polymerization in the presence of a template molecule. Once the template is removed, the resulting cavities are complementary in shape, size, and functional groups to the target molecule, enabling selective rebinding. Moreover, MIPs can be engineered to respond to external stimuli, such as temperature, thereby enabling controlled molecular recognition. MIPs have gained increasing attention due to their robustness, stability, low cost, and reusability, offering advantages over natural recognition elements such as antibodies and enzymes. These properties make them attractive for a wide range of applications, including biosensing, drug delivery, environmental monitoring, and chromatographic separations.

These polymers are created through Molecular Imprinting Technology (MIT), which was defined ‘The construction of ligand selective recognition sites in synthetic polymers where a template (atom, ion, molecule, complex or a molecular, ionic or macromolecular assembly, including micro-organisms) is employed in order to facilitate recognition site formation during the covalent assembly of the bulk phase by a polymerization or polycondensation process, with subsequent removal of some or all of the template being necessary for recognition to occur in the spaces vacated by the templating species’ in early studies [2]

MIT has gained widespread use across a broad range of scientific disciplines, offering innovative solutions for the selective recognition and removal of specific molecules. As a synthetic strategy, MIT enables the development of robust molecular recognition materials that mimic the behavior of natural receptors such as antibodies and enzymes. Its significance lies in the ability to create tailor-made materials with recognition capabilities comparable to those of biological systems. [3]

MIT is notably versatile, allowing for the selective recognition of a wide array of chemical and biological targets, including amino acids, proteins, nucleotide derivatives, environmental pollutants, pharmaceuticals, and food-related compounds.

The fabrication of MIPs involves the formation of a pre-polymerization complex between a target molecule and a functional monomer. This complex undergoes polymerization in the presence of a cross-linking agent, resulting in a stable three-dimensional polymer matrix. Following polymerization, the template is removed, leaving behind highly specific recognition sites that are complementary in size, shape, and chemical functionality to the original molecule. [3] The selective rebinding of the target molecule is primarily governed by non-covalent interactions such as hydrogen bonding, dipole–dipole forces, and ionic interactions. [3]

In essence, MIT allows for the creation of artificial receptors with high selectivity and specificity for their target analytes. Compared to natural recognition elements, MIPs offer superior physical and chemical stability, resistance to harsh environmental conditions, and long-term operational durability. Furthermore, their relatively low production cost and sustained performance under ambient conditions make them highly suitable for a wide range of practical, scalable, and long-term applications.

MIPs represent a synthetic alternative to natural receptors, combining biological-like recognition with enhanced mechanical, thermal, and chemical robustness.

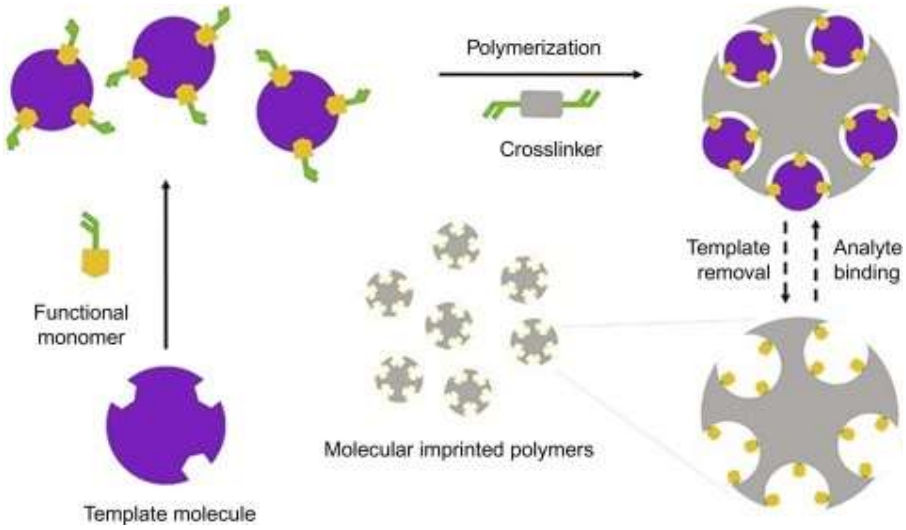

Figure 1.1 Scheme of Molecular Imprinting process [4]

This thesis explores the synthesis, characterization, and application of MIPs, with a particular focus on their versatility in imprinting two structurally and chemically distinct target molecules: Oxytetracycline (OTC) and Bovine Serum Albumin (BSA). OTC is an antibiotic widely used in the agricultural sector, whereas BSA is a large protein molecule. Due to their fundamentally different molecular properties, the imprinting of these two targets requires polymers with significantly different characteristics. This work aims to analyze the differences in the imprinting strategies for OTC and BSA, thereby highlighting the adaptability and versatility of MIT in designing selective recognition materials for diverse analytes.

1.1. Hard MIPs vs Soft MIPs

MIPs are synthetic materials engineered to contain specific binding sites tailored to a target molecule. As previously mentioned, molecular imprinting involves the formation of a pre-polymerization complex between the template molecule and functional monomers. Polymerization is then carried out in the presence of a crosslinking agent and a suitable solvent, which plays a crucial role in determining the final polymer morphology and microporous structure. Once the template is removed, the resulting polymer is a matrix with specific recognition sites complementary to the original template molecule. [5]

The structural and functional properties of MIPs are influenced by several factors, including the chemistry of the monomers (anionic, cationic, neutral, or amphiphilic), the type and strength

of interactions between monomer units and pendent groups, and the choice of solvent. In most imprinting techniques, site fidelity can be compromised due to macromolecular chain relaxation or swelling phenomena. To address this, high ratios of crosslinking agents to functional monomers are often used to minimize flexibility and maintain the structural integrity of the imprinted sites.

As the degree of crosslinking increases, the polymer network becomes more rigid, preserving the spatial arrangement of functional groups. In contrast, in less crosslinked systems, the spacing and conformation of these groups can shift as the network swells or contracts in response to the rebinding solvent. MIPs with a high crosslinking ratio, typically around 70%, are referred to as Hard MIPs, characterized by their mechanical stability and fixed cavity structures. Conversely, MIPs with a much lower crosslinking content, usually below 20%, are classified as Soft MIPs. Notably, studies by Wulff [6] and Mosbach [7] have demonstrated that it is possible to achieve specific molecular recognition even with crosslinking levels below 20%, challenging the traditional notion that high crosslinking is always essential for imprinting efficiency.

1.1.1. Structural and functional differences

Hard MIPs are the most well-known and widely used type of molecularly imprinted polymers. Characterized by a high degree of crosslinking, they possess a rigid and stable polymer matrix. This rigidity ensures that the imprinted cavities retain their specific shape and size even after template removal, which is important for maintaining high selectivity towards the target molecule. Due to their structural stability, they are particularly suitable for applications requiring mechanical robustness. However, the removal of the template can be time-consuming, and in many cases, achieving complete removal of the analyte can be difficult or even impossible.

Soft MIPs, which are most commonly hydrogels, are typically synthesized using water-soluble monomers. [8] These polymers exhibit a swelling behavior that can be finely tuned, allowing for controlled uptake and release of the template molecule. This responsive swelling helps to overcome limitations related to mass transfer and enhances effective rebinding.

Soft MIPs are usually composed of a major stimulus-responsive monomer that governs the swelling and shrinking behavior of the hydrogel matrix, and a minor functional monomer that interacts with the target molecule via multipoint electrostatic interactions. During synthesis,

the template and functional monomers self-assemble into a low-energy, three-dimensional configuration, with the functional groups embedded within the flexible polymer chains.

Unlike Hard MIPs with rigid, inflexible matrices, the functional groups in soft MIPs can dynamically reorient in response to external stimuli (e.g., pH, temperature, or ionic strength), enabling a controllable binding and release mechanism. The three-dimensional structure of the hydrogel provides a recognition site architecture that mimics the imprinted state, although this 'memory effect' may diminish when exposed to external stimuli. [8]

Soft MIPs have shown promising potential for the imprinting of biomacromolecules, owing to their inherent biocompatibility and stimuli-responsive properties. Despite technical challenges, molecular imprinting within hydrogels holds considerable promise for advanced applications in drug delivery and biosensing. Future developments are expected to enhance the selectivity toward target molecules and improve the ability of the gels to respond dynamically to their concentrations.

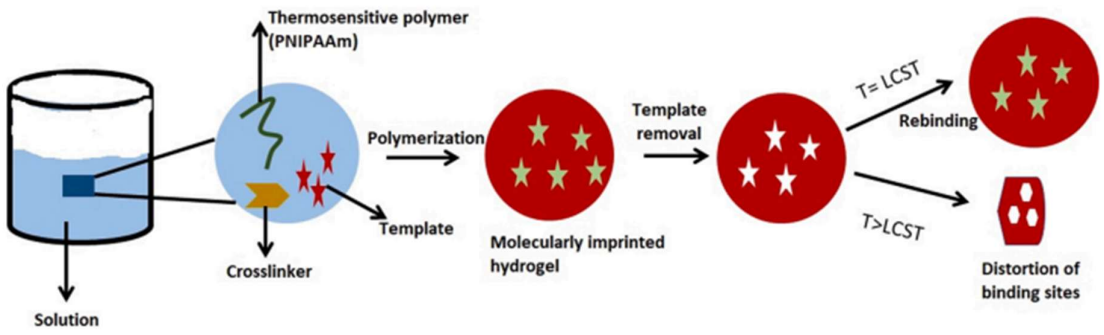

Figure1. 2 Illustration of thermosensitive behavior of polymer with lower critical solution temperature. [8]

1.2. Key Components of MIP Formulations

In the following paragraphs the main components of MIP will be examined in detail, with particular attention to their roles and effects in the formation of these polymers.

1.2.1. Template molecule

The primary goal of molecular imprinting is to create a polymer network with high affinity and selectivity toward specific template molecules. The template directs the formation of recognition sites by guiding the spatial arrangement of functional monomers during polymerization, resulting in the formation of three-dimensional cavities that are

complementary in shape, size, and functional groups to the template. [9] Additionally, the template must not contain functional groups that could inhibit the polymerization process. This ensures that the polymerization proceeds efficiently and that the monomers and crosslinker form a stable, cross-linked network around the template, enhancing the robustness and specificity of the resulting imprinted polymer. Template molecules can generally be categorized into four groups [10]:

1. **Ions** (e.g., Cd^{2+}, Cu^{2+}, Pb^{2+}, Hg^{2+}, CH_3Hg^+)
2. **Organic molecules** (e.g., pesticides, explosives, pharmaceuticals, endocrine-disrupting chemicals, amino acids and peptides, sugars—some examples are shown in Fig. 2)
3. **Biomacromolecules** (e.g., adenosine, bovine serum albumin)
4. **Cells and viruses** (e.g., bovine leukemia virus)

The best results have been achieved with substances having molecular weights between 200 and 1200 Da. Imprinting large macromolecules continues to be a significant challenge. [1] Larger templates are more flexible and may not facilitate the creation of well-defined binding sites during the imprinting process. Furthermore, the secondary and tertiary structures of macro biomolecules such as proteins, can be affected when they are subjected to the thermal or photolytic treatments involved in the synthesis of MIPs. [1]

1.2.2. Functional monomer

One of the most critical factors in molecular imprinting technology is the proper selection of the functional monomer, which directly interacts with the template molecule. During polymerization and subsequent cross-linking, this interaction leads to the formation of cavities that are complementary in shape and chemical functionality to the chosen template.

The functional monomer is responsible for the stability and robustness of the resulting MIP. The type of functional monomer determines the chemical nature of the recognition sites, while its concentration influences the number and density of binding sites. Typically, functional monomers are used in excess relative to the template molecule (commonly at a molar ratio of 4:1) to favor the formation of stable template–monomer complexes.

The chemical properties of the functional monomer (e.g., acidic, basic, hydrophobic, or hydrophilic groups) directly affect the specificity and affinity of the MIP. In fact, a crucial step in MIP synthesis is the identification of a suitable functional monomer capable of forming strong and selective interactions with the template.

According to Le Chatelier's principle [11], increasing the concentration of functional monomers or enhancing the binding strength within the pre-polymerization complex can lead to a greater number of high affinity binding cavities, thereby improving the selectivity of the final polymer.

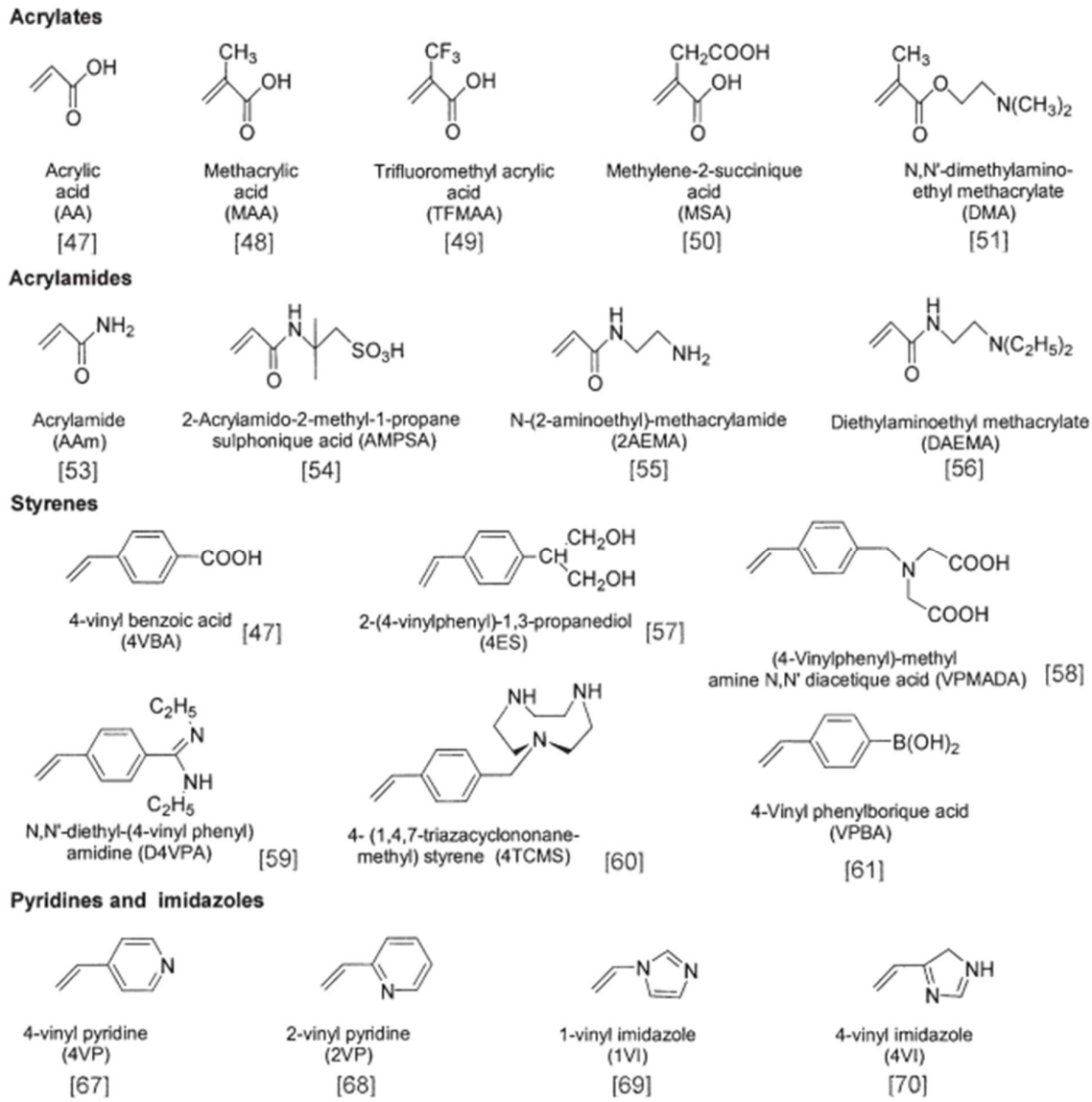

Figure1. 3 The monomers most used in MIP [12]

1.2.3. Cross-linker: rigidity vs flexibility of the polymer network

The cross-linker is a critical component in molecular imprinting, as it forms a three-dimensional network structure around the template–monomer complex. During polymerization, it stabilizes the orientation of functional monomers by creating a rigid matrix that encapsulates the complex. The cross-linker provides both mechanical and chemical stability to the resulting polymer, significantly influencing the morphology, mechanical properties, selectivity, and binding capacity of MIPs. [13] The degree of cross-linking plays a key role in determining the selectivity and structural stability of the MIP. Typically, a cross-linker content of over 70% is required to obtain a stable, porous material with a rigid matrix, as seen in "hard" MIPs. In contrast, "soft" MIPs are synthesized with lower cross-linker concentrations, resulting in a more flexible structure.

However, while a high degree of cross-linking enhances mechanical strength and structural integrity, it can also rigidify the polymer network, negatively affecting the diffusion kinetics of the target molecule. This may lead to reduced accessibility of the imprinted sites, thereby limiting the efficiency of template extraction and rebinding. [12] The number of vinyl functional groups per molecule in the cross-linker also influences the final polymer's mechanical properties and binding efficiency. For instance, MIPs synthesized using trimethylolpropane trimethacrylate exhibit greater mechanical stability and binding performance compared to those prepared with ethylene glycol dimethacrylate. [13]

Moreover, studies have shown that in MIPs based on non-covalent interactions, only about 10% of the generated binding sites are effectively active. [6]

In conclusion, the choice of cross-linker must be carefully considered based on the desired characteristics of the final MIP, including rigidity, porosity, and compatibility with both the functional monomers and the template molecule.

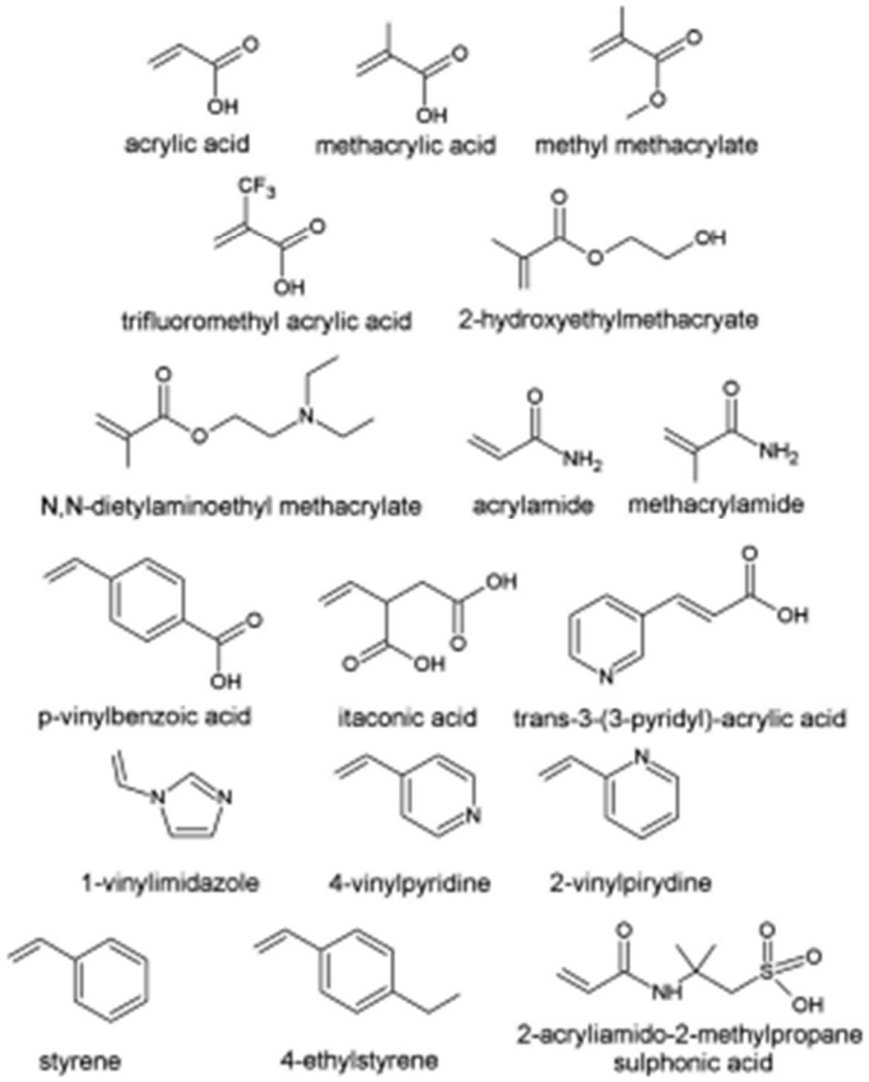

Figure 1. 4 Functional monomers used in the synthesis of MIPs [13]

1.2.4. Solvent: role in the imprinting process

The primary role of the solvent is to dissolve the template and monomer, thereby facilitating the formation of the pre-polymerization complex. It ensures a homogeneous distribution of all components within the reaction mixture, preventing the formation of aggregates during polymerization. The polarity of the solvent significantly influences the formation of the template–monomer complex; thus, the solvent plays a critical role in molecular recognition and acts as a dispersion medium throughout the reaction [14] For example, polar protic, aprotic, and non-polar solvents can modulate these interactions, thereby affecting the

efficiency with which the template directs the spatial organization of the functional monomers. [15]

The choice of solvent depends largely on the chemical nature of the template: polar solvents are more suitable for polar templates, while non-polar solvents are preferable for non-polar templates.

In addition to its role in solubilizing components, the solvent also functions as a pore-forming agent, influencing the polymer's morphology, porosity, and pore size. It is important to consider how the solvent affects the polymer network through swelling processes, as excessive swelling may reduce the polymer's rebinding capability. Optimal rebinding performance is generally achieved when the same or a chemically similar solvent is used during both the imprinting and rebinding processes, highlighting the importance of maintaining consistent solvation conditions. [14]

1.2.5. Initiator

The polymerization initiator plays a crucial role in starting the polymerization process, enabling monomers to react with each other and with the cross-linker. Initiators can be activated through thermal energy, UV radiation, or other methods. The majority of MIPs are typically synthesized via free radical polymerization, electropolymerization, or photopolymerization. [16]

Initiators generate free radicals, cations, or anions that initiate the polymerization of functional monomers and the cross-linker. The type and concentration of the initiator can significantly influence the polymerization rate; therefore, careful control of these parameters is essential to ensure the formation of a homogeneous polymer structure. Furthermore, the initiator can affect the microstructure of the resulting polymer, including the degree of cross-linking and the distribution of monomers within the polymer matrix. [17]

There are several types of initiators, including the following:

- Radical Initiators: These are the most common and include substances such as ammonium persulfate (APS) and benzoyl peroxide (BPO). They generate radical species under mild conditions and promote radical reactions.
- Cationic and Anionic Initiators: These are less frequently used; they start the polymerization by generating cations or anions. Cationic initiators generate positively

charged species that activate monomers, which then propagate the polymer chain through successive reactions. Similarly, anionic initiators generate negatively charged species that initiate polymerization.

The choice of initiator depends on several factors, including the type of monomers, the desired reaction conditions, and the target properties of the MIP. An efficient initiator ensures that the polymerization proceeds rapidly and completely, minimizing the presence of unreacted monomers and enhancing the overall quality of the final polymer.

1.3. Debinding and Rebinding Processes

According to the state of the art, debinding and rebinding processes are crucial for achieving optimal performance in MIPs. These steps depend significantly on the nature of the template and the characteristics of the resulting polymer. [18]

1.3.1. Template removal: challenges and techniques

Debinding (or washing) refers to the process of removing the template molecule from the MIP after polymerization. This step is essential for creating recognition cavities that allow the MIP to selectively rebind the target molecule.

Complete removal of the template is difficult to achieve, even after multiple washing cycles. This can be attributed to the limited accessibility of solvents to highly crosslinked regions or the solvent's insufficient solubility to disrupt interactions within the imprinted cavities. [19]

When dealing with large molecules or proteins, up to 25% of the original template may remain embedded in the polymer matrix [20] [21], which can significantly reduce MIP efficiency by decreasing the number of available binding sites. [18]Additionally, harsh or prolonged washing conditions may distort or destroy the imprinted cavities, ultimately impairing the MIP's selectivity and recovery performance. [22]

A proper comparison between MIPs and their corresponding non-imprinted polymers (NIPs) is essential. Notably, the NIP must also undergo the same washing process; skipping this step may lead to unrealistically high selectivity factors for the MIP. [23]

Common solvents used for template removal include acids, bases, organic solvents, and aqueous solutions. [18]
The following sections describe some extraction methods reported in the literature:

Incubation with Solvents

The simplest and more common technique for template removal involves immersion of MIP samples in an appropriate solvent. This method uses organic solvents such as ethanol, methanol, acetone, or acetonitrile to solubilize and remove the template from the polymer. [24]They exhibit good template solubility to break the interaction with the binding cavity and can induce the swelling of the network of the polymers.
This process is performed under mild conditions and does not compromise the chemical stability of the polymer [24]. It typically requires large solvent volumes and can be accelerated by heating or agitation. Solvent is replaced several times, and the amount of template released is monitored after each extraction cycle. [18]
The main advantage of this technique is its simplicity and straightforward experimental setup. However, it has several disadvantages, such as:

- Time-consuming (may require several hours or days).
- The method loses effectiveness when applied to templates that are difficult to solubilize.
- Generates significant solvent waste.

Conventional Soxhlet Extraction

Soxhlet extraction, introduced over 135 years ago, is a standard method and it is commonly used as the reference to compare the performance of other methods.
Finely ground MIP particles are placed into a porous cartridge within the Soxhlet extractor. The solvent used is usually an organic solvent containing acid or base additives and is poured into a flask connected to the lower end of the extractor chamber. The solvent is then heated, vaporized into the extractor chamber, then condensed vapor drops and enters in contact with the samples. The process is a continuos extraction. [18]

The solvent carrying the dissolved template descends through a siphon to the flask when a certain volume of liquid is achieved.

The main advantages are:

- Hot solvent improves template solubility.
- Continuous washing with fresh solvent
- Affordable equipment and easy to learn.
- Suitable for most polymer matrices.
- No post-extraction filtration needed

However, several disadvantages can be mentioned:

- Long extraction time (6-24h)
- Risk of template degradation at high temperatures.
- High amount of organic solvents used, which may raise ecological issues.
- Static sample conditions can slow extraction efficiency.

Pressurized liquid extraction

Also known as Accelerated Solvent Extraction, this method became commercially available in 1995 [25].

During this procedure, the samples are placed in a stainless-steel filled with the solvent.

The extraction is conducted at controlled temperature and pressure for 5-10 min and then the solvent is delivered to a collector. Nitrogen purging follows each cycle before introducing new solvent for another extraction cycle. The extraction takes place at high temperature(50-200°C) and pressure (10-14MPa) to facilitate the penetration of the solvent. This method is rapid (10–25 minutes total), uses less solvent (~15 mL per 10 g of sample), and can be easily automated for high-throughput applications.

A relevant advantage of this technique is the versatility of solvents and mixtures that can be used for the extraction, making it suitable for the removal of almost any substance.

In fact, if the solvent chosen is water, the system becomes more environmentally friendly and economical, applying high temperatures (~300°C) and pressures (10-60 bar). As temperature increases, water becomes more effective in solubilizing compounds of medium and low polarity, resulting in efficient template extraction. [26]

Microwave assisted extraction (MAE)

The microwave (MW) energy is a nonionizing radiation with frequencies in the 300 MHz to 300 GHz range, causing ionic conduction and dipole rotation.

Two operational modalities can be performed [18]:

1. Pressurized MAE (PMAE): Uses closed MW-transparent vessels, filled with high dissipation factor (the ratio between the dielectric loss and the dielectric constant) solvents. The solvent absorbs the energy and the temperature rises, but the pressure inside the chamber prevents the boiling of the solvent.
2. Atmospheric MAE system, in open MW-transparent vessels, which is also named Focused Microwave-assisted Soxhlet extraction (FMASE) [27]. This technique employs low dissipation solvent and, so, only the template extracted increases its temperature. The extraction is carried out under mild conditions, and is suitable for thermolabile substance

Several factors influence the efficacy of microwave-assisted extraction (MAE), including MW power and exposure duration, temperature, solvent volume, and solvent type, which all have a direct impact on template solubility and polymer solvation.

Some of the advantages are:

- Shorter extraction time (from 3 min to 1 h) and reduced solvent use (25–50 mL).
- Higher efficiency than traditional methods.
- “Clean” technique with low environmental impact.

However, it has several disadvantages:

- High temperatures may degrade sensitive MIPs.
- Requires balance between efficiency and preservation of polymer structure.

Ultrasound assisted Extraction (UAE)

Ultrasound refers to cyclic sound waves with frequencies above 20 kHz. When applied to liquid media, ultrasonic energy induces cavitation—the formation, growth, and implosive collapse of microbubbles. This phenomenon causes mechanical erosion of the MIP surface, exposing new

areas and thereby enhancing mass transfer and facilitating the removal of the template. Cavitation also leads to localized increases in temperature (which improves solubility and diffusivity) and pressure (which promotes solvent penetration and molecular transport). Ultrasound can be applied using either ultrasonic baths or probes. While probe-based systems allow for more localized and effective treatment, they are more expensive and typically accommodate fewer samples per run [28]. It is also possible to set up a continuous solvent flow through the chamber containing the polymer, further improving extraction efficiency.

After the extraction process, MIPs are typically recovered by centrifugation or filtration. Due to the relatively moderate temperature increase induced by ultrasound, UAE is particularly suitable for thermolabile templates that cannot tolerate the higher temperatures used in Soxhlet extraction. Moreover, UAE offers shorter extraction times and reduced solvent dependency compared to traditional Soxhlet methods. [18]

Supercritical phase extrusion

Supercritical phase extraction involves the use of fluids that are above their critical temperature and pressure. In their supercritical state, these fluids exhibit gas-like viscosity and diffusivity while retaining liquid-like solvating power, making them highly efficient for template removal.

The process begins by pumping the supercritical fluid into an extraction chamber maintained at the appropriate temperature and pressure. Extraction can occur in various operational modes:

- **Static:** The extraction cell is filled and kept at equilibrium.
- **Dynamic:** The supercritical fluid continuously flows through the chamber.
- **Recirculating:** The same fluid is cycled through the chamber multiple times.

After extraction, the supercritical fluid is directed toward a trapping system where the extracted template is collected. [29]

The most used supercritical solvent is carbon dioxide [18], due to its low cost, low toxicity, and ability to easily reach supercritical conditions (above 32 °C and 73 atm). CO_2 is effective for a wide range of templates and enables gentle yet complete template removal.

The advantages of this method include reduced extraction time compared to other methods, lower use of organic solvents, and non-toxicity to the environment of the waste products of this process.

Subcritical Water Extraction

Water is the most economical and environmentally friendly ("green") solvent available. Its efficiency in template removal can be significantly enhanced under elevated pressure (10–60 bar) and temperature conditions (100–374 °C). [30]
This process is also referred to as **Pressurized Hot-Water Extraction (PHWE)** or **Superheated Water Extraction**. When water is heated under pressure, it undergoes a substantial reduction in polarity. This decrease in polarity allows water to dissolve a broad range of compounds, including polar, ionic, and even non-polar substances. Additionally, the concurrent reduction in surface tension and viscosity significantly enhances both diffusivity and mass transfer rates. The thermal energy applied during SWE can disrupt non-covalent interactions such as van der Waals forces, hydrogen bonds, and dipole–dipole interactions, both between solute molecules and between the solute and the polymer matrix. Meanwhile, the applied pressure forces water into otherwise inaccessible regions of the polymer structure. The SWE unit is quite simple and consists of a water reservoir, a medium-pressure pump, an oven, and a restrictor. It can be coupled online with different techniques. The main limitation of the technique, which can be carried out in static and dynamic modes, is that it is not suitable for labile templates or for polymer matrices that cannot withstand high temperatures. [18]

1.3.2. Rebinding of target analytes: mechanisms and efficiency

This paragraph aims to explore the current state of the art regarding the rebinding process in Molecularly Imprinted Polymers (MIPs), in which specific recognition cavities, created during the imprinting phase, selectively rebind the target molecule. This process demonstrates both the selectivity and recognition efficiency of the MIP toward its template.
The main steps involved in the rebinding process are:

- **Target Exposure**: The MIP is exposed to a solution containing the target analyte. The analyte molecules diffuse toward the recognition cavities embedded within the polymer matrix.
- **Specific Interactions**: The target molecules bind to the recognition sites through various interactions, such as hydrogen bonding, van der Waals forces, hydrophobic effects, and electrostatic interactions. At this stage, the nature of the polymer plays a critical role: in **hard MIPs**, the rigid, highly crosslinked structure resulted in having limited flexibility slowing the rebinding process, while **soft MIPs**, which are less crosslinked or hydrogel-based, provide more dynamic and adaptable binding environments that facilitate faster analyte access.
- **Binding Equilibrium**: The process reaches equilibrium, where a defined fraction of the analyte is bound within the MIP cavities, while the rest remains in solution.

The most commonly used method to evaluate and achieve analyte rebinding is batch rebinding**.** In this approach, the MIP samples are dispersed in a solution containing the target analyte. Due to the presence of highly specific recognition sites, the polymer is able to absorb again the analyte. To improve mass transfer and contact between polymer and analyte, the whole system can be agitated via a tilting or shaking platform. The advantages of this method include its simplicity, precise control over analyte concentration, and adjustable incubation time. However, limitations may arise from solubility issues of either the polymer or the analyte, which can hinder effective rebinding.

Analyte-Dependent Rebinding Considerations

The rebinding behavior differs significantly depending on the nature of the target analyte:

- For small molecules, rebinding is primarily governed by basic physicochemical factors such as molecular size, polarity, and site affinity. The process is generally fast, predictable, and less influenced by environmental parameters. Challenges may arise from cross-reactivity with structurally similar molecules. [31]
- For proteins or larger biomolecules, the rebinding process becomes more complex and sensitive. Factors such as solution pH, three-dimensional conformation, and electrostatic interactions play a dominant role. pH, in particular, can affect the structural integrity and binding behavior of the protein, with denaturation or aggregation

posing significant risks to rebinding efficiency. As a result, protein rebinding is typically slower, less predictable, and more prone to non-specific interactions or reduced capacity due to structural alterations of the target. [31]

2. MIP Fabrication: Traditional and Alternative Methods

Molecularly Imprinted Polymers (MIPs) are synthetic engineered to contain specific biding sites for a target molecule. The synthesis of these materials typically involves three main steps:

- **Formation of the pre-polymerization complex**: Functional groups of the monomer interact strongly with those of the template molecule to form a stable complex. In essence, the monomer is organized around the template through thorough mixing. A solvent is often used at this stage to facilitate the dissolution and interaction of the components.
- **Polymerization**: A crosslinking agent and a polymerization initiator are added to the mixture. Upon heating or exposure to UV light, polymerization occurs, and the crosslinker forms a three-dimensional polymer matrix around the pre-polymerization complex.
- **Template removal (debinding)**: In the final step, the template molecule is removed, leaving behind binding sites within the polymer matrix. These sites are complementary in shape, size, and chemical functionality to the original template, enabling selective recognition and binding.

It' s important to specify that the initial stage of interaction between the template and functional monomer, can be performed using different approaches. The functional monomers can form complex with a template through covalent and non-covalent interactions.

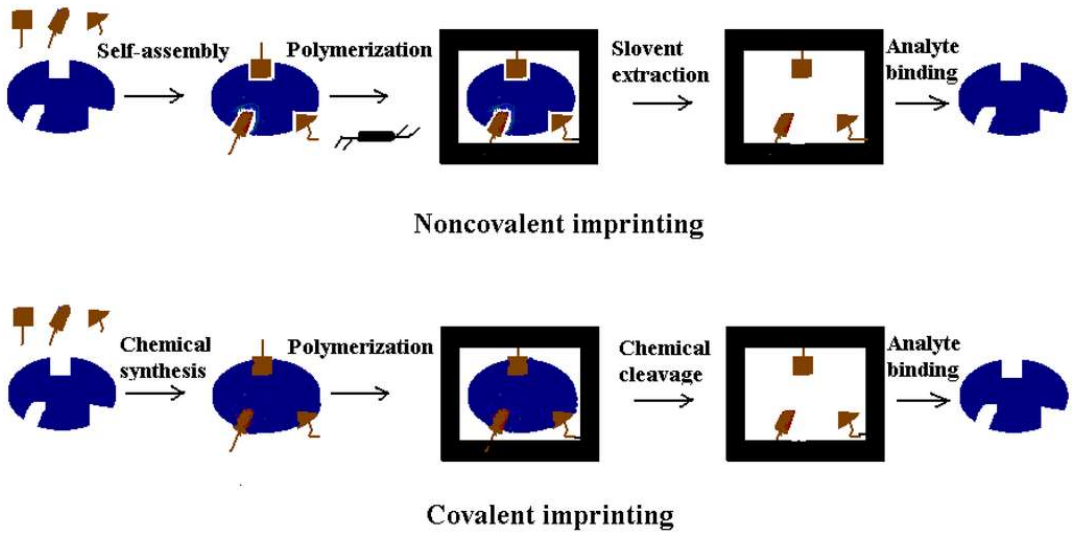

Figure2.1 Schematic representation of covalent and non-covalent molecular imprinting procedures [32]

Covalent approach:

In covalent approach, the imprinted molecule is covalently coupled to a polymerizable molecule. The strategy involves the formation of reversible covalent bonds. [32] During polymerization, this bond is maintained, and only after polymerization is it broken to remove the template. Reversible covalent interactions with polymerizable monomers are fewer in number and often require an acid hydrolysis procedure to cleave the covalent bonds between the template and the functional monomer. [32]

This approach aims to reduce non-specific binding. Some drawbacks include the complexity of template removal, which may require aggressive conditions potentially damaging to the polymer. [9]

This method requires controlled reaction which may limit its versatility. It is useful when very high selectivity is required, provided that specific and controlled reaction conditions can be handled.

Non-covalent approach:

The non-covalent approach depends on ionic interactions, hydrogen bonding, van forces, π-π interactions between the template molecule and the function monomer. This is the most common method due to its simplicity and rapidity of the method. In fact, non-covalent protocol is easily conducted, the removal of the template Is generally much easier, usually accomplished by continuous extraction. The non-covalent imprinting approach seems to hold more potential for the future of molecular imprinting due to the vast number of compounds, including biological compounds, which are capable of non-covalent interactions with functional monomers. [33] [34]

Semi-covalent approach:

In the semi-covalent approach, the formation of the complex between the template and the functional monomer is based on covalent interactions, but the interaction between the template molecules and imprint cavities is via noncovalent bonds. [35] The synthesis of MIPs in this case is more difficult since it has to ensure that non-covalent interactions are strong enough for template recognition after its removal, but at the same time the template removal is generally simpler than in the pure covalent method.

The semi-covalent approach has the benefit of covalent and non-covalent methods. It combines the high selectivity of imprint cavities that are made by covalent imprinting with the speed of binding the target molecules to the imprint cavities of non-covalent interaction. [36]

In conclusion, the choice of the approach depends on the selectivity and specificity of MIPs for the desired application, the manageable reaction conditions, and the complexity of the synthesis.

2.1. Conventional synthesis approaches

In the state of art, the are many synthesis methods and some of them are going to be explained in the following paragraphs. These synthesis methodologies can apply to all three primary approaches for binding the template molecule to the functional monomer in Molecularly Imprinted Polymers.

Free radical polymerization

Free-radical polymerization (FRP) is the most common methos to synthesize MIPs. It can be performed in a wide range of temperatures since it can be initiated thermally and photochemically as well [37]. It's very tolerant to functional groups in the monomers.

The mechanism includes three distinct stages:

- Initiation: Initiator (via heating or UV/visible irradiation) generates free radicals
- (R•), which are very active because they have unpaired electrons. They react with the monomer (M) generating an initiating radicals chain (R-M•).
- Propagation: The main phase of polymerization, where the chain grows through the addition of monomer molecules to the growing macroradical (R-Mn•), transferring its active center to the attacked molecule.
- Termination: The growth of macromolecules chain stops and the polymerization terminates by disabling the active center. The two most common termination mechanisms in radical polymerizations are combination and deprotonation. The first one consists of combining two radical chains to form a single macromolecule. The second one involves the transfer of a hydrogen atom from one chain to another, leading to one macromolecule

Although FRP is widely used for the synthesis of MIPs, it does not allow for the control of the size, architecture, and number of growing macromolecules. [13]

MIPs obtained by classical FRP, controlled and living radical polymerization can be prepared by bulk, suspension, emulsion, precipitation or multi-step polymerization. [13]

Bulk

Bulk polymerization is quick and simple which requires the use of template, functional monomer, cross-linker, initiator and porogen. It is performed in solution, followed by lyophilization or drying. Then the materials are crushed and sieved. The particles obtained this way have irregular size and shape. This technique is characterized by poor reproducibility and selectivity. [13]

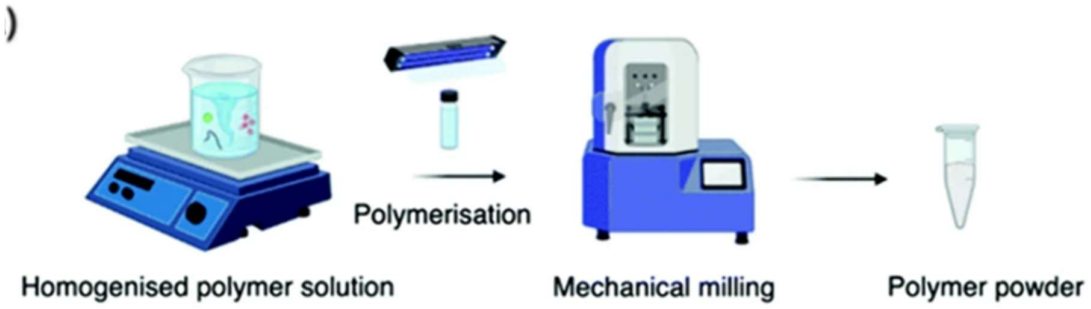

Figure 2.2 Bulk polymerization [39]

Suspension polymerization

Suspension polymerization is also a simple method, with one step polymerization that allows to permit to obtain spherical particles but characterized by having a large dimensions (in the range from micrometres to milimetres). This polymerization typically occurs in water medium, but other continuous phases such as perfluorocarbon liquids and mineral oils can also be used. [13] Due to influence of dispersing medium the MIPs produced exhibit poor recognition. Suspension polymerization is one of the technique that can be applied on a large scale. [13]

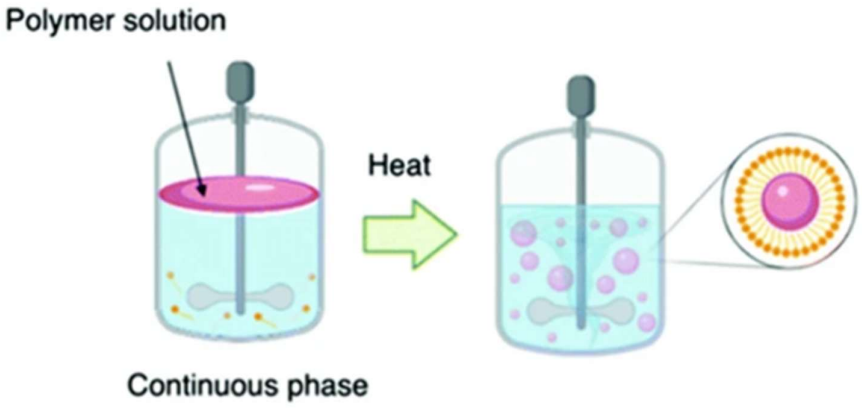

Figure2.3 Suspension polymerization [39]

Emulsion polymerization

Emulsion polymerization is a high yield polymerization method in which a prepolymerization mixture containing the initiator (polar phase), is suspended in an oily solvent (non-polar phase) with a surfactant, The surfactant acts as a template for producing spherical micellar MIPs. The resultant MIPs can be used in various applications, including drug delivery, catalysis, and as selective filters in chemical sensors and chromatographic separations. [38]

Emulsion polymerization permits to obtain monodispersed polymer particles. Polymer particles usually are in the size range of tens to hundreds nanometres. In this type of polymerization water is typically used as the continuous phase. Water due to strong polarity and hydrogen bonding capability and surfactants can affects the efficiency of the imprinting process by influencing the stability of the interactions between template molecule and functional monomers impacting the imprinting process. Because of this emulsion polymerization is not widely used for the synthesis of MIPs. [13]

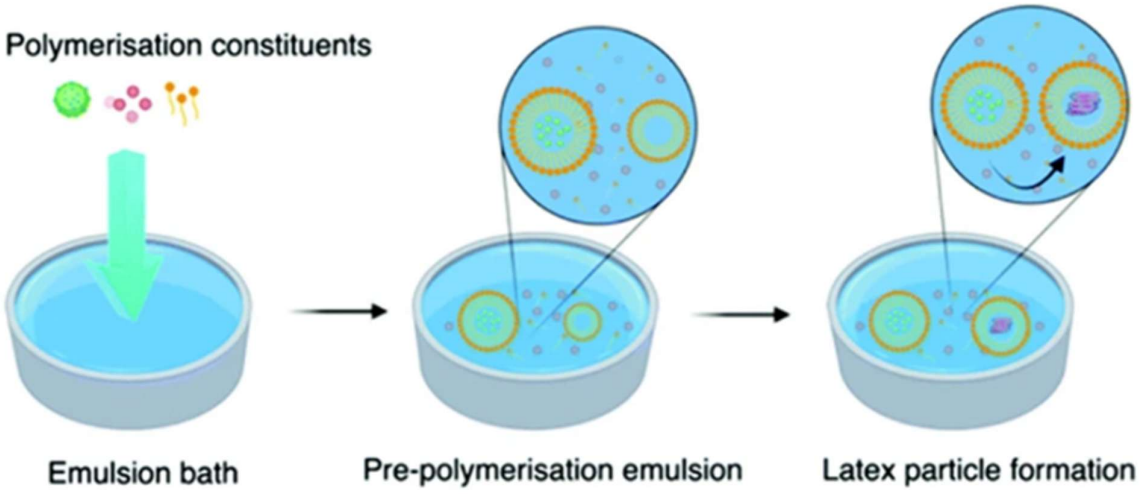

Figure 2.4 Emulsion polymerization [39]

Precipitation polymerization

Precipitation polymerization is a procedure that requires just one step. This method produces uniform and spherical particles (diameters usually less than 1μm) but need the use of a large amount of template. [13]Precipitation polymerization is a surfactant-free method, which involves polymerization of monomers in dilute solutions without overlap and coalescence, and resultant polymer particles will precipitate from the solution. [13]

Precipitation polymerization requires a large amount of solvent. Several factors influence the size of obtained particles, such as polarity of the solvent, reaction temperature and speed of stirring, so it is important to controls the reaction conditions. [13]

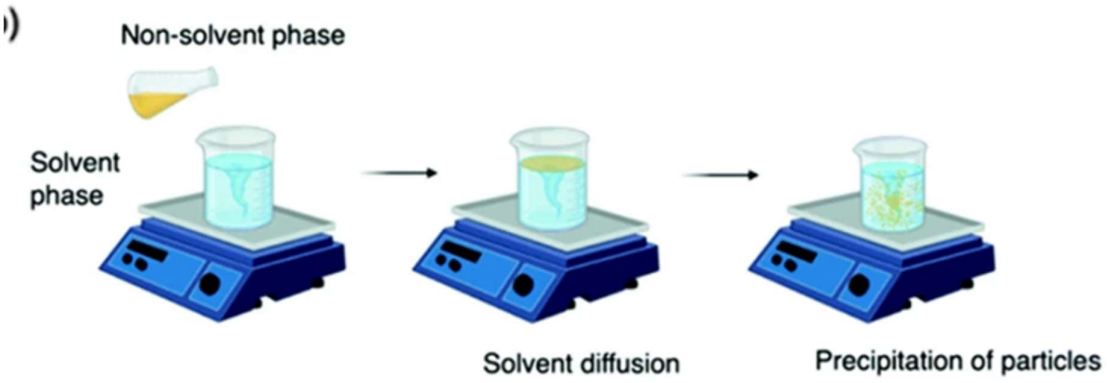

Figure 2.5 Suspension polymerization [39]

Surface imprinting polymerization

Surface imprinting polymerization involves surface grafting of thin MIP layer onto prepared beads. The products obtained are monodisperse. It is a time-consuming method and the results can be used in separation of sensing applications in the form of thin imprinted layers. The recognition sites are formed near to the surface of the material, making them more accessible, making the removal of the template easier.

There are two main types of surface imprinting:

• **MIP films** are formed by depositing a thin layer on different substrates via spin-coating or deep-coating methods then a stamp is pushed into a partly polymerized film and kept in place until the film fully polymerizes. Binding sites are left on the MIP film surface after removing the stamp and template molecules.

• **core-shell particles** that are produced using water-in-oil (W/O) emulsion polymerization. The particles cores are coated with thin MIP layer. The initial stage is to synthesize the core material, which is typically silica particles, or it could be made of magnetic particles. It is responsible for providing stability to core-shell MIP particles. Subsequently there is the polymerization of the polymer to form a shell around the core particles. These approaches demonstrate the adaptability and specificity of surface imprinting in creating highly efficient MIPs for sophisticated applications.

Multi-step swelling polymerization

Multi-step swelling polymerization (also called seed polymerization) is a time-consuming complicated procedure. Seed particles are swollen in water with functional monomers, crosslinker, template and initiator. The monomer diffuses into the seed particle, enlarging it. This can be done in multiple swelling steps to carefully control particle growth and size uniformity. Once the swelling is complete, polymerization is initiated.

This method permits to obtain monodisperse spherical particles that can be prepared in the form of beads of controlled diameter and controlled porosity. The MIPs obtained are well fitted for the chromatographic applications, solid-phase extraction, and chemical sensing, underscoring its broad applicability and success in polymer research. [13]

2.2. Fundamentals of photopolymerization

The photopolymerization reaction starts when a light-sensitive system, photoinitiator, in its ground state undergoes electronic transition to an excited state upon light irradiation, and then active reactive species, which usually are free radicals or ions are created. These active species interact with the functional monomers, initiating chain reactions that lead to the formation of polymers. Depending on the nature of the reactive species the polymerization can be categorized in free radical, cationic, anionic polymerization. [40]

Radical photopolymerization reactions consist of three steps: initiation, propagation, andtermination. In the initiation step, light activates the photoinitiator, radicals are generated. Then they interact with monomers to form monomeric radicals. During the following step, these monomeric radicals react with additional monomers, leading to a chain reaction. The termination step occurs when the reaction ceases, typically when two growing chains meet, and the radicals are inactivated. [40]

The ionic photopolymerization mechanism is characterized by using reactive species in the form of ions, often cations, to trigger and propagate the polymerization reaction. A significant advantage is not being sensitive to oxygen, having low film shrinkage and better adhesion on the substrate. The main drawbacks are its high sensitivity towards water and its lower kinetic rate compared to free-radical photo-polymerizations. Additional heat treatment after light-curing is often required to improve monomer conversion.

The 3D printing method based on photopolymerization technique requires the use of photocurable resins, which are composed primarily by photoreactive precursors and photoinitiators, but it could even contain additives, absorbers, and fillers to enhance performance. [40]

The precursors are monomers, or prepolymers that solidify upon exposure to light, forming the resin's matrix and determining the final properties of the printed object. The photoinitiators react with light to initiate the polymerization process. Additives such as dyes, inhibitors, and diluents are used to improve the resin's quality and control the printing process. Absorbers help to prevent over-polymerization. Fillers can modify the printed material's physical and mechanical properties.

2.3. 3D Printing as an Innovative Fabrication Method for MIPs

2.3.1. Introduction to 3D printing

3D printing, also known as additive manufacturing (AM) or rapid prototyping, includes a range of technologies able of printing three-dimensional objects through layer-by-layer deposition of materials. Unlike subtractive manufacturing where the final object is obtained by removing materials from the initial block, additive manufacturing builds the objects progressively by adding material, layer by layer, until a specific geometry is achieved. Due to adding material only where needed there is a significant reduction in material waste and environmental impact. AM is considered an emerging technology that is driving innovations across design, materials science, and engineering. It offers the potential to reduce production costs and waste while increasing design flexibility and overall manufacturing efficiency. [41]

When using polymeric materials, AM can be successfully implemented with a wide variety of polymers in different formulations, including composites, nanocomposites, continuous or discontinuous fiber-reinforced thermoplastics, and hybrid materials. [41]

One of the major advantages of AM is the ability to fabricate complex three-dimensional geometries that would be difficult or impossible to produce using conventional techniques. Moreover, AM platforms can support multi-material printing, enabling the fabrication of functional components or composites. In the biomedical field, this versatility is especially valuable, as AM enables the production of patient-specific tools, prostheses, implants, and devices, which can significantly improve clinical outcomes and patient comfort.

Despite its many advantages, AM still faces several challenges that hinder its full-scale industrial adoption. These include:

- Dimensional limitations in fabricating large-scale components,
- Surface roughness and imperfections resulting from the layer-by-layer process,
- High initial investment costs for advanced AM equipment and high-performance materials.

In general, a 3D printing workflow consists of five structured steps:

1. Design: A detailed 3D model of the object is created using Computer-Aided Design (CAD) software. Alternatively, existing physical objects can be digitized through technologies such as Magnetic Resonance Imaging (MRI), laser scanning, or Computed Tomography (CT).

2. File conversion: The CAD model is exported to an STL (Standard Tessellation Language) file format, which approximates the object's surfaces using a mesh of triangles. The number and size of these triangles influence the resolution and fidelity of the printed object.
3. Slicing: Specialized software converts the STL model into a series of horizontal layers, generating the G-code, a set of machine instructions that defines parameters such as layer height, print speed, extrusion temperature, and print orientation.
4. Printing: Once the G-code is loaded into the 3D printer, the actual fabrication begins. The object is built layer by layer according to the predefined path.
5. Post-processing: After printing, the object typically undergoes various post-processing treatments such as curing (for photopolymers), sintering (for powders), or cleaning and surface finishing, in order to meet final specifications in terms of mechanical properties, dimensional accuracy, and aesthetic quality.

2.3.2. Printing technologies: focus on DLP

Printing methods can be classified into three main groups [42]:

- **Extrusion-based techniques**: the filament passes through a heated nozzle and it transition from solid to a liquid state. This melting allows precise deposition of the material, which rapidly cools and solidifies. Fused Deposition Modeling (FDM) and Direct Ink Writing (DIW) are two of the methods that use this approach.
- **Powder-based techniques**: Thin layer of powders are deposited and subsequently pressed and compacted. These powders are then selectively melted using either a binder or laser radiation at desired locations. Selective Laser Sintering (SLS) exemplifies this approach, where powdered material is fused together in layers to create solid objects.
- **Photopolymerization-based techniques:** A resin composed of photopolymers and a photoinitiator undergoes rapid polymerization when exposed to appropriate light irradiation. In this category there are stereolithography and vat photopolymerization techniques, like Digital Light Processing (DLP), which allow the best resolution.

Digital Light Processing (DLP)

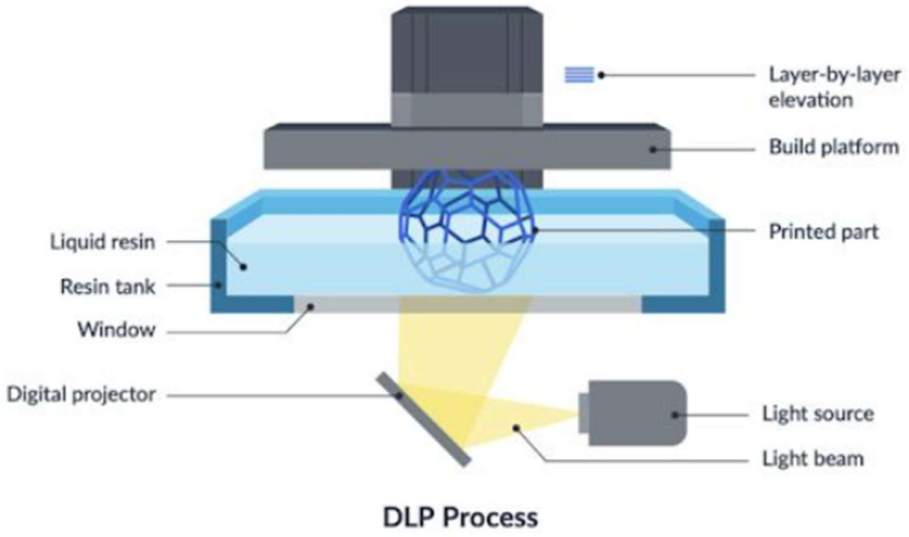

Figure 2.6 Digital Light Processing [83]

Digital Light Processing (DLP), also referred to as Projection Stereolithography, operates on a principle similar to that of traditional Stereolithography (SLA), with a few key differences in system architecture and light delivery. In DLP systems, the light source is positioned beneath the resin vat, while the build platform is suspended above the resin bath. Unlike SLA, which uses a rastering ultraviolet laser to cure the resin point by point, DLP utilizes a digital micromirror device (DMD)-based projector. This projector can illuminate and cure an entire layer simultaneously, significantly reducing the overall print time. [43]

DLP employs photopolymer resins with viscosities comparable to those used in SLA. It supports both free-surface and constrained-surface exposure configurations, offering similar advantages and facing similar limitations to SLA. [43]

Standard DLP systems typically use light sources with wavelengths around 365 nm or 405 nm and can achieve feature resolutions ranging from 10 to 50 microns, depending on the optics' magnification and the resolution (number of mirrors) of the DMD chip. This high level of precision makes DLP suitable for applications requiring fine detail, such as dental models, jewelry, and microfluidic devices. [43]

One of the primary advantages of DLP is its significantly faster printing speed, as entire layers are projected and cured in a single exposure. In addition, less resin is required compared to

traditional SLA systems, since the entire build volume doesn't need to be submerged in resin. This contributes to lower material costs and easier material management. However, there are also notable limitations to this technology. Because objects are formed within a uniform resin bath, each printed part is limited to a single material per print job, restricting multi-material applications. [42]

Furthermore, due to the pixel-based nature of DLP projection, curved surfaces may exhibit visible layer lines or "stair-stepping" artifacts. Achieving smoother surfaces and higher resolution requires a reduction in pixel size, which in turn may limit the maximum printable build volume. This occurs because the DMD has a fixed number of mirrors, and increasing resolution by shrinking pixels inherently reduces the size of the projected image. As a result, larger parts are often printed at a lower resolution than smaller ones to balance detail and build area.

Despite these constraints, DLP remains a powerful and efficient technology for producing highly detailed, small to medium-sized objects with rapid turnaround times.

2.3.3. Advantages and limitations of 3D-printed MIPs

One of the main limitations of molecularly imprinted polymers (MIPs) lies in their undefined architecture resulting from traditional synthesis methods. To address this issue, one promising solution is the use of additive manufacturing (AM) technologies, which are ideal for generating accurately defined three-dimensional structures while retaining the functional properties necessary for target molecule recognition. [44]

In a recent study, the digital light processing (DLP) 3D printing technique was successfully employed to fabricate complex MIP architectures for the sequestration of copper (II) ions. The resulting structures exhibited high affinity for copper ions, and the architecture supported efficient template removal. These results highlight how the integration of molecular imprinting and 3D printing represents an innovative and potentially scalable approach. [44]

Another notable example involves the use of two-photon stereolithography (TPS) to fabricate chemical sensors based on MIPs. This technique enables the creation of complex three-dimensional microstructures with sub-micrometric resolution. [45]

Additionally, one study reported the use of micro-stereolithography (μ-SLA) to produce MIP-based 3D microstructures capable of selectively recognizing adenine [46]. Subsequently, two more studies [45], [47] applied two-photon polymerization stereolithography (TPP-SLA) for similar purposes.

While TPP-SLA achieves extremely high resolution, its printing speed is relatively low. In contrast, μ-SLA offers faster printing and the ability to produce larger structures, albeit with lower resolution. Despite its improved speed, μ-SLA still faces significant limitations.

There is a pressing need to develop and optimize a 3D printing technique that can rapidly and efficiently fabricate MIPs with complex architectures and high functional performance.

The present thesis will focus on the fabrication and recognition capabilities of MIPs produced via DLP 3D printing, exploring its potential for high-resolution, scalable applications in chemical sensing and selective separation.

3. MIP Materials and Formulations: Hard vs Soft

3.1. Ingredients of Formulation

For the Hard MIPs Oxytetracycline hydrochloride, methacrylic acid, Phenylbis(2,4,6-trimethylbenzoyl)phosphine oxide (BAPO), and dimethyl sulfoxide and methyl red were purchased from Sigma-Aldrich (Milan, Italy). Dipropylene Glycol Diacrylate was purchased by Allnex.

For Soft MIPs Bovine Serum Albumin (BSA), N-Isopropylacrylamide (NIPAM), 2-Hydroxyethyl methacrylate (HEMA), Poly(ethylene glycol) diacrylate (PEGDA), 2-Acrylamido-2-methyl-1-propanesulfonic acid (AMPS) and 2-Hydroxy-4'-(2-hydroxyethoxy)-2-methylpropiophenone (Irgacure2959) were purchased from Sigma Aldrich (Milan, Italy).

3.1.1. Molecule Template

Oxytetracycline is the template used in this thesis for Hard MIPs; it is a tetracycline class antibiotic. The molecule was chosen because of its huge presence in agricultural, human therapy, and veterinary medicine. The administration of animals is the first step to a chain of events that not only causes environmental consequences but also supports the issue of antibiotic resistance. The drug is is expelled by the body through urine and feces in an active form, eventually polluting water drains Due to its resistance to biological degradation, conventional wastewater treatment is ineffective to remove OTC, and it is therefore emitted into the natural aquatic environment. [48]Tetracycline is harmful for algal communities, inhibiting growth of different algae in the concentration range 0.25–30 mg/L. It is not surprising that the higher the dose, the more profound the effects are. [49]

Antibiotic residues have also been found in cow's milk and in other food items that derives from animal, this could lead to negative health impacts on consumers, including allergic responses and endocrine abnormalities. Indeed, World Health Organization (WHO) and Food and Drug Administration (FDA) established a maximum residue limit of 0.1 mg L–1 and 0.3 mg L–1, respectively, for OTC in milk to protect human health. [50]

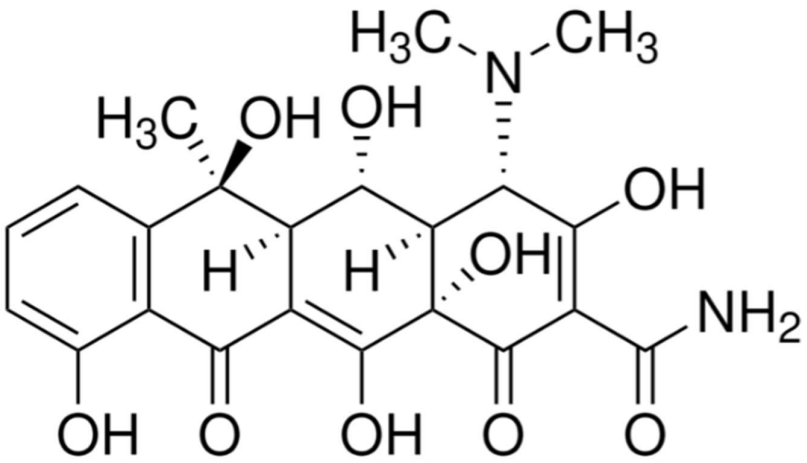

Figure 3.1 Chemical structure of Oxytetracycline [51]

For Soft MIPs Bovine Serum Album (BSA) has been selected as the template molecule. BSA is one of the most extensively studied proteins in the serum albumin family. It is a globular protein composed of 582 amino acid residues and is organized into three structurally homologous domains (I,II,III). It contains 20 tyrosine (Tyr), and two tryptophan (Try), which are situated in positions 134 (sub-domain IA) and 212 (sub-domain IIA). [52] [53]

BSA constitutes approximately 52-62% of the total protein content in blood plasma. [54] As a major plasma protein, albumin plays a crucial role in maintaining osmotic pressure and also functions as a carrier of small molecules, such as drugs, hormones, fatty acids, and metal ions [55].

Structurally, BSA is known for its remarkable flexibility, which allows it to adapt to environmental changes and to bind a wide variety of ligands. The reversible binding of numerous compounds, especially negatively charged molecules, makes BSA highly relevant in both transport and regulatory processes, with significant biological implications [56]. The isoelectric point (pI) of BSA lies between pH 4.5 and 5.0, meaning that at physiological pH (~7.4), BSA carries a net negative charge. [57] BSA is also characterized by its high solubility and stability, making it particularly suitable for use in various biochemical applications. When analyzed using UV-Vis spectroscopy, BSA exhibits a characteristic absorption peak at 278 nm, which is primarily due to the presence of aromatic residues, especially tryptophan and tyrosine. [53]

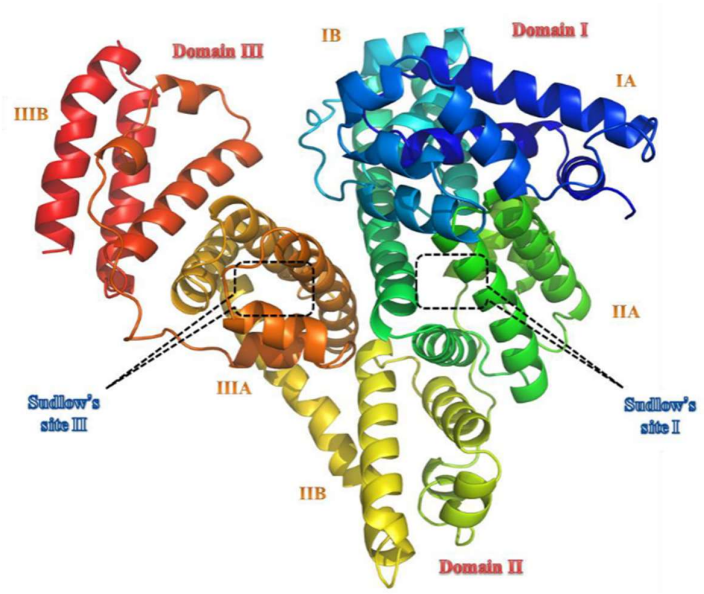

Figure 3.2 Illustration of Bovine Serum Albumin [58]

3.1.1 Functional monomer

The functional monomer employed in the formulation for Hard MIPs is methacrylic acid. Due to the presence of carboxyl groups that can form hydrogen bonds with the target molecule, it exhibits a high affinity for the template. In the literature, most MIPs created through non-covalent imprinting use methacrylic acid as functional monomer. [32]

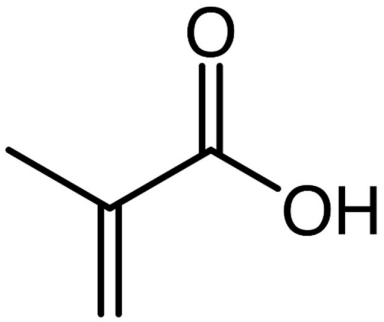

Figure 3.3 Chemical structure of Methacrylic acid [59]

For the formulation of Soft MIPs the monomer used are three:

- N-Isopropylacrylamide (NIPAM) is a biocompatible monomeric unit that can be used in the creation of stimuli responsive polymers. One of its main features is its temperature-sensitive behavior, which is governed by its lower critical solution temperature (LCST), around 32 °C in aqueous solutions. Below this temperature, NIPAM-based polymers are

hydrophilic and swell in water, while above the LCST, they undergo a reversible phase transition to a more hydrophobic, collapsed state. This thermoresponsive characteristic makes NIPAM ideal for applications such as drug delivery, tissue engineering, and smart biomaterials. [60]

- 2-Acrylamido-2-methylpropane sulfonic acid (AMPS) is a reactive and hydrophilic monomer and belongs to the class of sulfonic acid acrylic monomers. AMPS has an ionic character due to the sulfonic acid group, which is valuable for applications such as ion exchange, flocculation, and water treatment. Its strong hydrophilicity and ionizable functional group also make it particularly effective in the synthesis of superabsorbent hydrogels, where it contributes to enhanced water uptake and swelling capacity. Incorporation of AMPS into hydrogel networks significantly improves their superabsorbent performance, making it a valuable component in biomedical, agricultural, and hygienic product applications. [61]
- 2-Hydroxyethyl methacrylate (HEMA) is a hydrophilic monomer with great biocompatibility. It is a viscous clear, soluble, colorless liquid, with a pungent, sweet odor, and exhibits high reactivity due to its methacrylate group, readily undergoing polymerization. Its homopolymer is water-insoluble but plasticized and swollen in water. The presence of the hydroxyl group in its structure enhances water absorption, crosslinking potential, and adhesion, making HEMA suitable for medical applications. [62]

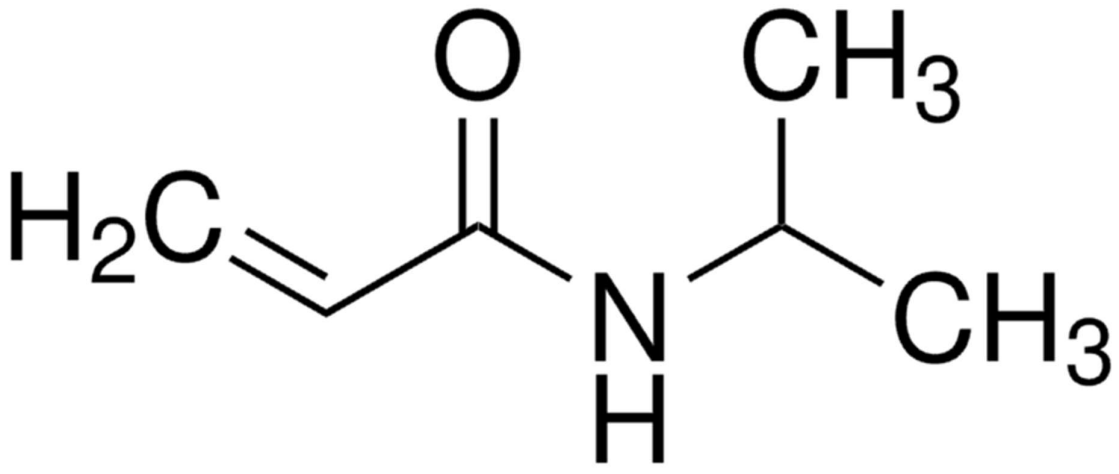

Figure 3.4 Chemical structure of N-Isopropylacrylamide (NIPAM) [63]

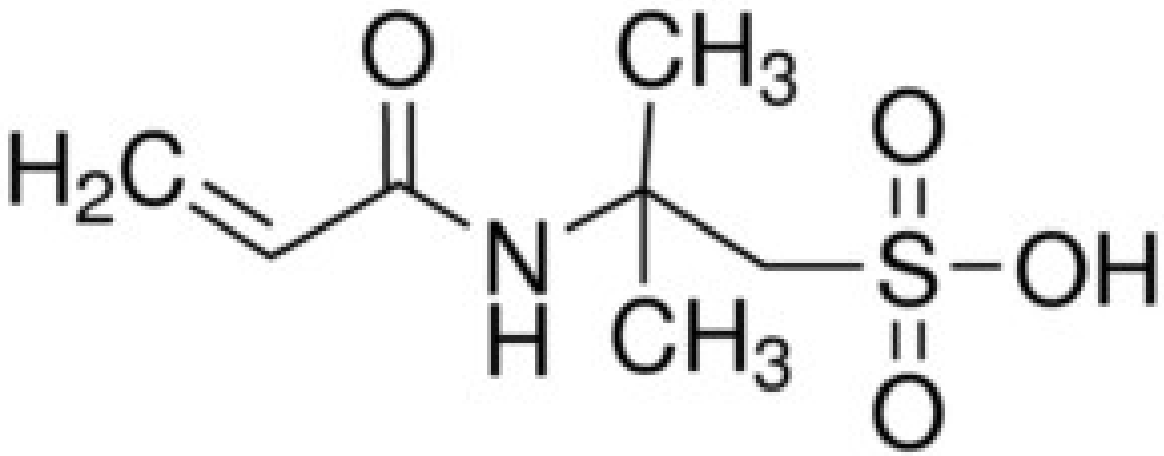

Figure 3.5 Chemical structure of 2-Acrylamido-2-methyl-1-propanesulfonicacid (AMPS) [61]

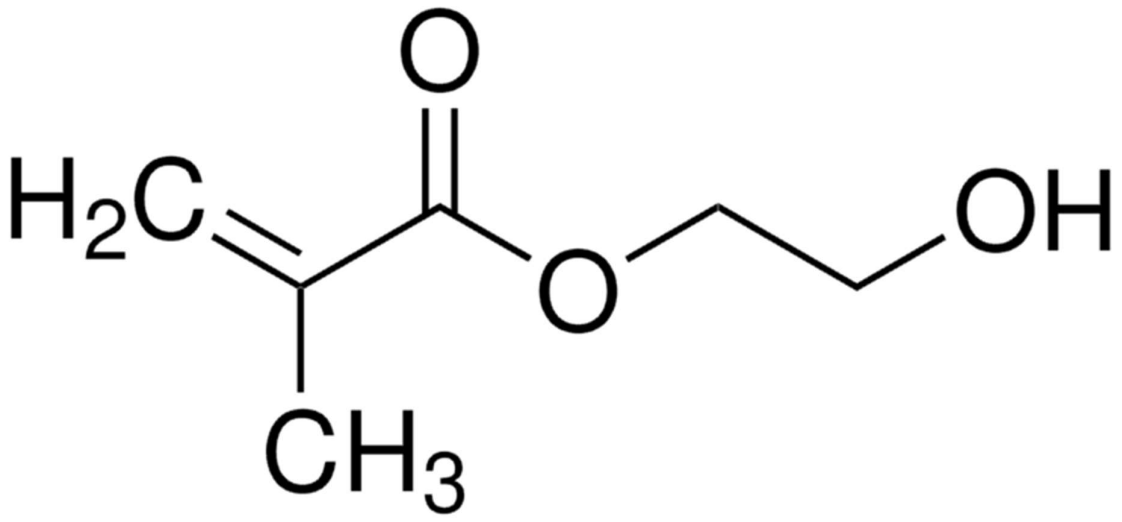

Figure 3.6 Chemical structure of 2-Hydroxyethyl methacrylate (HEMA) [62]

3.1.2 Crosslinker

Dipropylene Glycol Diacrylate (DPGDA) was chosen as the crosslinker for the formulation of MIP having OTC as the target molecule. It presents two reactive acrylate groups and it's compatible with a wide spectrum of functional monomers used in MIP formulations. DPGDA presents low viscosity, making it easier to mix and handle pre-polymer solutions [64]. This monomer was chosen over more traditional crosslinkers for MIP due to the better performance in 3D printing. In fact, DPGDA didn't show cracking due to shrinkage stresses after 3D printing, keeping a good balance between the ability to form the cavity structures, maintaining sufficient

swellability and flexibility to allow solvent permeation during the binding and debinding steps. [65]

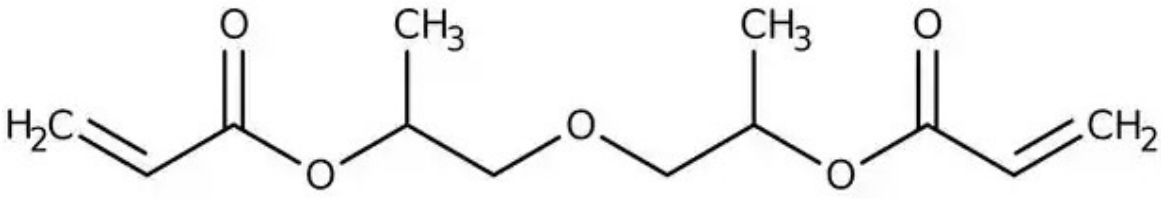

Figure 3.7 Chemical structure of Dipropylene Glycol Diacrylate (DPGDA) [66]

Poly(ethylene glycol) diacrylate is the crosslinker chosen for the second formulation. PEGDA is a derivative of polyethylene glycol and is a bifunctional acrylate monomer used in the synthesis of hydrogels, coatings and crosslinked polymer networks. Its hydrophilic nature and tunable mechanical properties make it ideal for biomedical, adhesive, and 3D printing applications. [67] By selecting PEGDA with a defined chain length, it is possible to fine-tune these properties within resin formulations, enabling precise control over the mechanical and structural characteristics of the final printout.

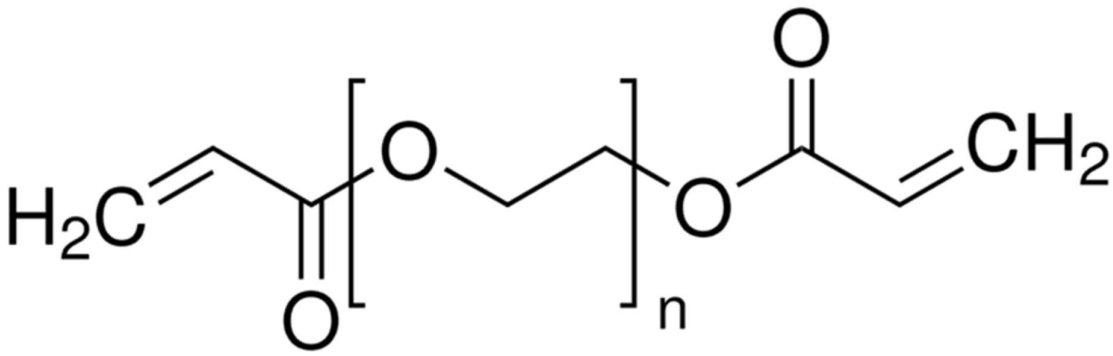

Figure 3.8 Chemical structure of PEGDA [68]

3.1.3 Solvent

The solvent chosen for the Hard MIP formulation is dimethyl sulfoxide (DMSO). DMSO is a polar aprotic solvent, relatively inert, nontoxic and stable at high temperatures. [69]The solvent, having a high boiling point, allows the polymerization process to take place at high

temperatures without evaporating. Having a high dielectric constant, it allows to dissolve many monomers, crosslinkers, and templates, thereby creating a homogeneous pre-polymer solution essential for forming a uniform polymer network. [70]

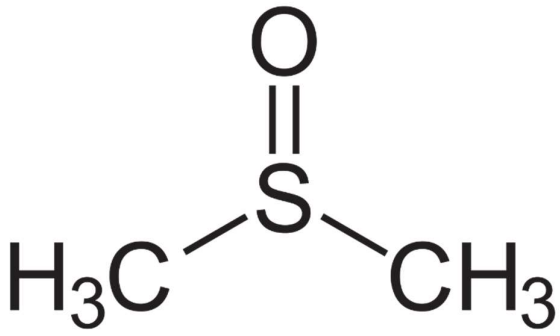

Figure 5.9 Chemical structure of dimethyl sulfoxide (DMSO) [71]

Instead, for the Soft MIP formulation, deionized water is used as the solvent. Deionized water is produced by removing almost all dissolved minerals ions such as sodium, calcium, iron, copper from the initial water, typically through ion exchange process. The resulting solvent is characterized by low electrical conductivity, a neutral pH, and the absence of taste or odor. Additionally, deionized water possesses a high relative dielectric constant (approximately 80), making it well-suited for facilitating polar interactions and promoting effective dissolution of ionic or polar species in formulation system.

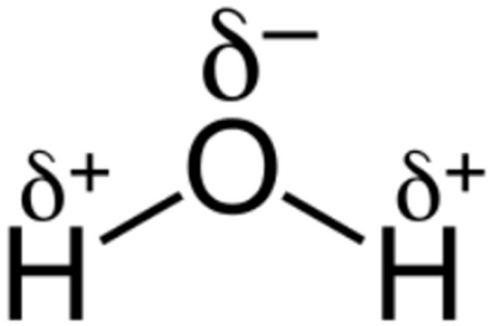

Figure 3.10 Chemical structure of water [72]

3.1.5 Photoinitiator

For the formulation having OTC as target molecule the chosen photoinitiator is phenylbis(2,4,6-trimethylbenzoyl) phosphine oxide (BAPO). The polymerization mechanism is triggered by the

absorption of UV light, which causes the cleavage of the phosphine oxide bond. This process generates reactive free radicals that initiate the polymerization of monomers. The primary molecular targets are the double bonds in acrylate and methacrylate monomers, leading to the formation of cross-linked polymer networks. [73]This compound presents thermal stability, solubility, compatibility with resin components, favorable safety profile, and ability to facilitate rapid and controlled polymerization, characteristics needed for successful 3D printing processes.

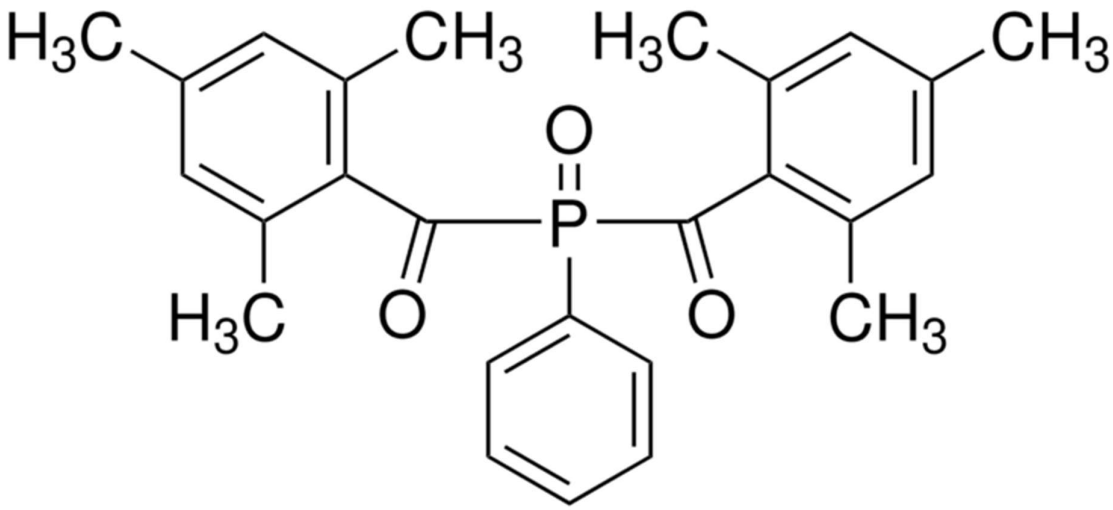

Figure 3.11 Chemical structure of phenylbis(2,4,6-trimethylbenzoyl) phosphine oxide (BAPO)

Instead, for the formulation having BSA as target molecule 2-Hydroxy-4'-(2-hydroxyethoxy)-2-methylpropiophenone has been chosen as the photoinitiator. This compound, commonly known as Irgacure 2959, has a high-purity UV photoinitiator optimized for crosslinking of methacrylated hydrogels in 3D bioprinting. Activation starts with UV light at 365 nm, it facilitates controlled photopolymerization, ensuring precise gelation, enhanced structural stability, and minimal cytotoxicity. Due to its water solubility, it is well-suited for aqueous-based formulations, such as those involving PEGDA or other hydrophilic monomers.

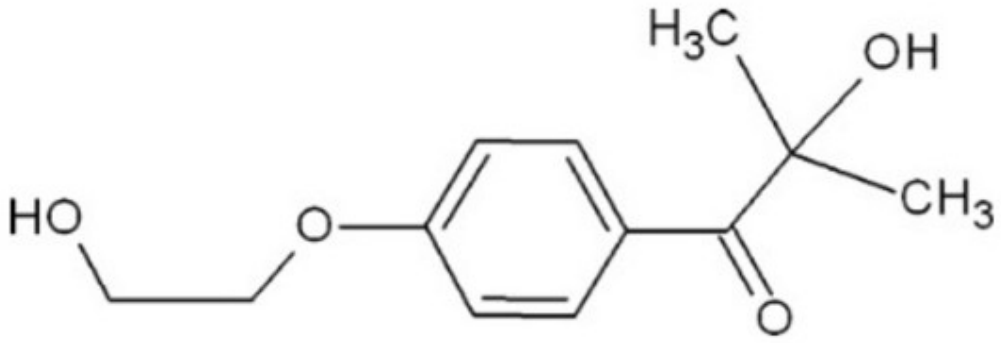

Figure 3.12 Chemical structure of 2-Hydroxy-4'-(2-hydroxyethoxy)-2-methylpropiophenone (Irgacure2959)

3.1.6. Dye

The use of dye was necessary to enhance the printability of the NIP formulation. Indeed, it minimizes scattering and helps concentrate light in a specific direction. The chosen one was methyl red.

Methyl red (2-(N,N-dimethyl-4-aminophenyl) azobenzenecarboxylic acid), also called C.I. Acid Red 2, is an azo dye, or a synthetic dye, that turns red in acidic solutions. Methyl red is red when the pH level is below 4.4, yellow when pH is above 6.2, and orange when the pH is somewhere between these two limits. [74]

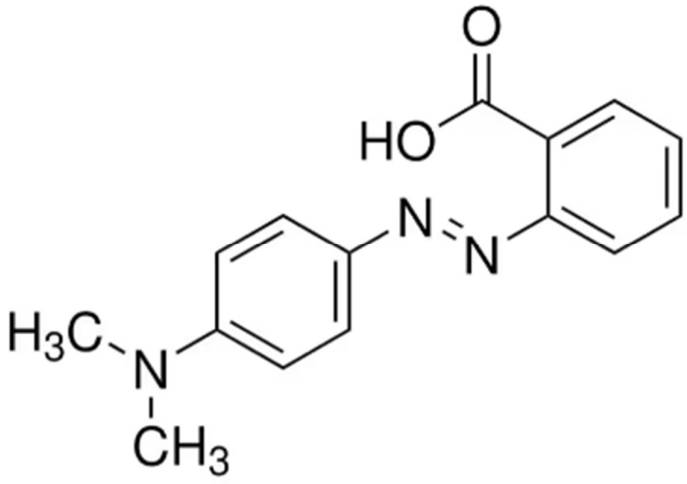

Figure 3.13 Chemical structure of methyl red [75]

3.2. Preparation of the Formulation

3.2.1. MIP resin: Molecularly Imprinted Polymer for OTC

This thesis employs the non-covalent approach as the binding strategy between the template and the functional monomer. The MIP formulation was prepared according to the following weight ratios between template (OTC), functional monomer (MAA) and crosslinker (DPGDA):

MIP → OTC: MAA: DPGDA = 1:5:20

Then 15 phr (per hundred resins) of solvent (DMSO) and 1 phr of photoinitiator (BAPO) were added.

The preparation of the resin consists of three main steps:

- The first step involves preparing the polymeric precursors by mixing DPGDA with BAPO, followed by placing the mixture in an ultrasonic bath for at least ten minutes or until the photoinitiator is fully dissolved
- The next step consists of the preparation of the pre-polymerization complex by combining OTC, MAA and DMSO. To be able to ensure the self-assembly between the functional monomer and the template, the compounds are mixed with magnetic stirring at approximately 600 rpm for at least one hour
- The last step consists in mixing the two previously prepared components by gradually adding dropwise the polymeric precursors to the complex containing the template. This has to be done while maintaining magnetic stirring at approximately 700 rpm. If a suspended phase forms, the stirring speed should be increased.

At the end of the procedure, it is necessary to ensure that the final resin is completely transparent and homogeneous. If not, it should be sonicated for an additional 10 minutes. The formulation must be clear to confirm the effective dispersion of all the ingredients.

3.2.2. NIP resin: Non-Imprinted Polymer

NIP formulation is essential for analyzing the difference between specific and nonspecific adsorption. To facilitate this comparison, the NIP resin contains all the components of the MIP

resin, except for the template, thereby preventing the formation of cavities typical of molecularly imprinted polymers.

The ingredients are the functional monomer, crosslinker, photo initiator and solvent, with the same weight percentages as the MIP resin, with the addition of 0.01phr of dye.

The preparation of the NIP formulation consists of two main steps:

- "Polymeric precursors" preparation as for MIP resin.
- Mixing MAA, DMSO and methyl red and addition to the precursors.

Since complete solubilization of the OTC is not required, the precursors don't need to be added gradually under magnetic stirring.

3.2.3. MIP resin: Molecularly Imprinted Polymer for BSA

The formulation for Soft MIPs using BSA as target molecule was prepared according to the following weight ratios between template (BSA), functional monomers (NIPAM, HEMA, AMPS) and crosslinker (PEGDA575):

MIP → BSA: (NIPAM, HEMA, AMPS): PEGDA = 12.85%:(76.95%:7.04%:1.54%):1.62%

To this formulation, 20 phr (per hundred resins) of solvent (deionized water) and 1 phr of photoinitiator (Irgacure2959) were added.

The preparation of the resin consists of two main steps:

- BSA is first dissolved in the deionized water under magnetic stirring at a low speed (approximately 50 rpm) to minimize foam formation. Since BSA tends to adhere to the walls of the container, it is important to carefully monitor the mixing process to ensure complete dissolution and uniform distribution of the protein.
- After the BSA has fully dissolved, the functional monomers, the crosslinker (PEGDA575), and the photoinitiator are added to the solution. The mixture is then stirred magnetically at approximately 600 rpm for about 1 hour. As with the first step, continuous monitoring is necessary to ensure that all components are fully dissolved and well-integrated.

At the end of the process, the final resin must be visually and physically homogeneous to confirm the effective dispersion of all ingredients.

3.2.4. NIP resin: Non-Imprinted Polymer

As already said, the NIP formulation is essential for evaluating the difference between specific and nonspecific adsorption. To enable this comparison, the NIP resin includes all the components of the MIP resin, except for the template (BSA), thereby preventing the formation of specific binding sites.

The ingredients are the functional monomer, crosslinker, photo initiator and solvent, with the same weight percentages as the MIP resin.

The preparation of the NIP formulation involves a single step. All the compounds are mixed using magnetic stirring at approximately 600 rpm. Since no protein (BSA) is present to dissolve, the mixing process is significantly faster and requires approximately 20 minutes. The final result is a homogeneous and clear solution, indicating complete dispersion of all components.

3.3.1. DLP 3D Printer

In this thesis, the Hard MIPs samples are fabricated using 3D printing via photopolymerization. The ASIGA MAX UV-X27 printer is employed for this process, utilizing Digital Light Processing (DLP) technology, which enables high resolution and precise detailing in the printed structures. The printer is equipped with a 385 nm LED UV light source. The printer is controlled through its proprietary software, ASIGA Composer, which allows for the precise adjustment of all printing parameters. It offers a resolution of 27 µm on the x-y plane and 1–500 µm along the z-axis.

The build platform measures 51.8 x 29.2 mm^2 and can produce objects up to 75 mm in height. The platform operates vertically, from bottom to top, with the sample printed in reverse.

3.3.2. Printing Process, Cleaning and Post-Curing of Hard MIPs

The samples were printed with a specific geometry known as "gyroids," 1.2 mm in height, selected for their high surface area relative to their compact volume. The printing process involved placing approximately 1 mL of resin into the printer tank and carefully optimizing the

printing parameters for each distinctive range. Key parameters that were thoroughly investigated included the layer thickness, light intensity, and exposure time for each printing layer. The first printing phase, referred to as the "burn-in", ensures proper adhesion of the sample to the printing platform. Following this, additional ranges may be applied depending on the selected geometry and resin type.

After the printing parameters were optimized, multiple samples were produced, and several post-processing steps were carried out once the samples were removed from the platform:

- **Cleaning:** The printed samples were immersed in a solvent, such as ethanol or isopropanol, and inserted in a sonication bath for 1–2 minutes to remove excess resin from the parts.
- **Post-Curing:** Following cleaning, the samples were dried with laboratory paper and then exposed to UV light to complete the polymerization process. This step enhances the material's properties, such as strength and hardness. Post-curing was performed for 3 minutes on each side using the Asiga® Flash Cure Box. After this, the samples were ready for testing.

3.3.3. Printing Process of Soft MIPs

In this thesis, the formulation of Soft MIPs is still in its early stages and has not yet been optimized for the 3D printing via Digital Light Printing (DLP) technology. A preliminary material test was performed using the ASIGA MAX UV-X27 printer. The test revealed phase separation within the resin, characterized by a more aqueous phase settling at the bottom and a crystallized phase forming at the top. As a result, polymerization was carried out using the Asiga® Flash Cure Box for 20 minutes. This method allowed the preparation of samples despite the limitations encountered with the 3D printing approach.

3.4. Debinding, rebinding

3.4.1. Debinding o washing: washing conditions

To remove completely during the washing step, the samples were placed in a flask and immersed in the washing solution. The flask was positioned on a tilting platform to facilitate

effective cleaning through the movement of the fluid. The washing solution was refreshed every few hours, and each time it was replaced, the samples were sonicated to enhance the extraction process. This procedure was repeated until the template was fully removed.

The washing solutions used to remove the template molecules from the MIPs were selected based on the chemical nature of the target compounds. For MIPs containing OTC, a solution of acetic acid (AA) and methanol (MeOH) in a 1:9 volume ratio was used. In contrast, for MIPs synthesized with BSA as the template, the washing solution consisted of deionized water (H_2O) supplemented with sodium chloride (NaCl) at a concentration of 100 mmol/L.

To ensure that the NIP samples underwent the same conditions as the MIP samples, it was decided to apply this exact process to NIP samples, even though they do not contain the template molecule.

3.4.2. Rebinding process of Hard MIPs: experiment setup

After the samples were washed, they were incubated in a solution containing the template used in the imprinting process to assess the ability of the binding sites to capture the target molecules. The amount of template remaining in the solution after binding to the polymer was measured and compared to the initial concentration. This comparison yields a dimensionless percentage parameter that describes the sample's removal capacity.

$$\%\ Removal\ = \frac{(Ci\ -\ Cf)}{Ci} * 100$$

Where:

- ***Ci*** is the concentration (µM) of the initial rebinding solution
- ***Cf*** is the concentration (µM) measured in each time step of the rebinding experiment

In this work, the rebinding solution is composed of OTC dissolved in demineralized water, prepared at known concentrations. Both MIPs and NIPs samples were tested. At different time steps the solution was analyzed using the UV-Visible plate reader to determine if the samples had successfully captured the template. The absorption spectrum of the rebinding solution collected was compared to the spectrum of the initial solution, with particular attention to the 355 nm wavelength, which corresponds to the characteristic absorption peak of the template

molecule. The ideal outcome is a gradual decrease in the absorption peak over time, relative to the initial value. The final step involved determining the concentration values using a calibration curve and calculating the removal percentage based on previously described parameters.

3.5. Characterization Methods

This paragraph will present and analyze the various methodologies used to characterize both the liquid resins and the printed samples.

3.5.1. Rheology

Rheology is a branch of physics that describe the deformation and flow behavior of various types of materials. Rheometry is the technique used to determine rheological properties such as viscosity, storage modulus (G') and loss (G''). Viscosity measures a material's resistance to flow. The storage modulus (G') represents the elastic behavior indicating how much energy is stored during deformation, while the loss modulus (G'') represents the viscous behavior, indicating how much energy is dissipated as heat. [76]

The device used for these measurements is called a rotation rheometer. Rheometers can operate in two main modes: oscillatory rotation and continuous rotation. [76]In continuous rotation mode, the rheometer measures the material's response to shear stress by applying a constant rotational force to the sample. The output of this test is the flow curve, which represents the relationship between shear stress and shear rate. Several important rheological properties, such as viscosity, can be derived from this curve. Viscosity is a property that can vary with temperature, duration, or shear stress. [76]

Another important test is the analysis of temperature-dependent viscoelastic behavior. This test allows for an investigation of how a material's viscoelastic properties change as a function of temperature. It is particularly useful for studying the thermal behavior of polymers, gels, and resins. The test is conducted under constant frequency and strain, and the evolution of the storage modulus (G') and the loss modulus (G'') is monitored throughout the temperature range.

Studying the rheological behavior of a material allows for the optimization of processing methods, improvement of product stability and quality, therefore the viscosity (η) of

unpolymerized resin, for both MIP and NIP resins was measured as a function of shear rate ($\dot{\gamma}$) using the shear rate test. The measurements were performed using an Anton Paar MCR 302 rheometer, configured in parallel plate setup.

3.5.2. Photorheology

Photorheology studies how the rheological properties of a material change in response to light exposure, usually in the UV or visible spectrum. These changes may involved alterations in the material's viscoelastic behavior, polymerization kinetics, or other photoinduced processes.

In this thesis, an oscillatory time sweep test was employed to monitor how the viscoelastic properties of the formulation evolve over time under constant conditions. The aim was to investigate how the presence of the target molecule affects polymerization kinetics, by comparing MIP and NIP resins. During the oscillatory time sweep test, the frequency, strain amplitude, and temperature were kept constant. The test was conducted within the Linear Viscoelastic Region (LVER) to avoid structural damage to the material. To determine the LVER, an amplitude sweep test was performed previously.

In the amplitude sweep, the formulation is tested at a constant frequency while the oscillation amplitude is gradually increased. The storage modulus (G') and loss modulus (G'') are measured throughout the test and the LVER is identified as the range in which both G' and G'' remain constant. The strain amplitude for subsequent tests is selected to ensure it falls within this linear region. Beyond a certain point (the critical strain), the structure starts to break down: G' decreases indicating loss of elastic behavior and G'' may increase indicating increased viscous behavior.
When the material is in a liquid-like state usually G'' > G'. In contrast, in a solid-like state, G' > G''. During photo-crosslinking, the rheological curve typically shows:

- A progressive increase in both G' and G''.
- A crossover point (the gel point) where G' exceeds G'', marking the transition from liquid to solid. The gel point is important in applications like 3D printing, as it provides information into the required exposure time and helps optimize printing parameters.

The slope of the increase in G' and G'' reflects the rate of polymer network formation and the delay time, that is the interval between light activation and gel point, is associated with the initiation phase of the polymerization reaction. These rheological tests were performed at 25°C, using a parallel-plate configuration with a gap of 200 µm. For the analysis of temperature-dependent viscoelastic behavior the temperature investigated was from 10 °C to 50°C. A broad-spectrum Hamamatsu LC8 UV lamp was used as light source.

The photorheological test consisted of two main steps:

- Initial phase where G' and G'' values are monitored.
- Irradiation phase that starts after 60 seconds with activation of the lamp and continues for a defined period.

3.5.3. Wettability

The ability of a liquid to spread over or adhere to a solid surface is known as wettability, and it is an essential aspect in determining how the liquid and solid interact. The angle formed between a tangent plane to the liquid surface and a tangent plane to the solid surface at the point of contact is known as the contact angle, and it is frequently used to quantify this property. The degree to which a liquid spread on a surface can vary; better wetting and spreading of the liquid are indicated by a smaller contact angle. When the contact angle is zero, the liquid completely wets the surface without creating a noticeable droplet. This is known as perfect spreading. [77]

The contact line is the line of intersection of the three interfaces (liquid-solid, solid-vapor, liquid-vapor), where the following surface tensions act concurrently:

- The solid-liquid surface tension, directed inward toward the droplet;
- The solid-air (solid-vapor) surface tension, directed outward from the droplet;
- The liquid-air (liquid-vapor) surface tension, directed along the tangent to the droplet at the point of contact.

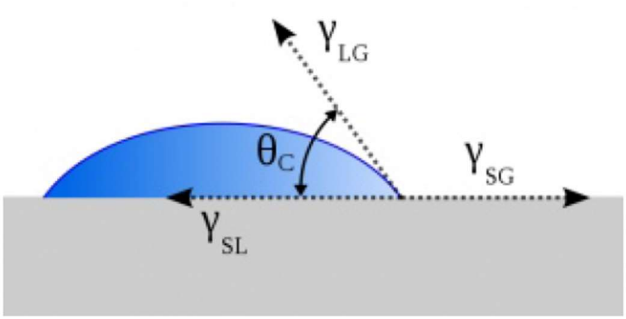

Figure 3.14 Droplet on a horizontal surface [84]

The equilibrium of these forces and the resulting contact angle are described by Young's equation.

$$cos\theta = \frac{\gamma_{sg} - \gamma_{sl}}{\gamma_{lg}}$$

The contact angle can vary over time. The static contact angle (SCA) refers to the contact angle measured when the system is at equilibrium on a horizontal surface. An isotropic surface is classified based on its interaction with water as follows:

- It is considered hydrophilic if SCA < 90°, indicating good wetting;
- Hydrophobic if SCA > 90°, indicating poor wetting;
- Superhydrophobic if SCA > 150°, where on the surface are formed nearly spherical droplet

According to numerous studies, the shape of the drop, the wetted surface area and the contact angle depend on the type and volume of deposited liquid, on the characteristics of the vapor that surrounds the drop and the surface, on the material (or materials) of which the surface is composed, and on the microscopic morphology of the surface (roughness, impurities, presence and alignment of fibers, etc.).

In this thesis, the instrument used to conduct this measurement is Biolin scientific Theta Lite.

3.5.4. UV/visible spectroscopy

UV-Vis spectroscopy is an analytical technique that measures the absorption over a determined range of ultraviolet (UV) or visible light. The absorption/transmission through a sample to the values of a reference or blank sample. This property is influenced by the sample composition, potentially providing information on what is in the sample and at what concentration. [78]This approach is widely used to determine the quantity of radiation absorbed or emitted by an analyte.

UV-Vis spectroscopy operates on the principle that the energy of matter is quantized, and photons of radiation can be absorbed or emitted by a substance if their energy matches the energy difference between allowed electronic transitions in the species. This interaction between electromagnetic radiation and matter results in the collection of spectra.

There are various spectroscopic techniques in the literature, each tailored to specific species, types of radiation-matter interactions, and regions of the electromagnetic spectrum.

In this study, UV-Vis spectroscopy was used to assess the rebinding capacity of the samples by indirectly measuring the absorbance of the solution in which the samples were immersed.

The Bouguer-Lambert-Beer law provides the mathematical foundation for determining light absorption in gases and solutions across the UV, visible, and infrared regions of the spectrum. [79]

$$A = log(Io \cdot I) = \varepsilon \cdot l \cdot c$$

From which derives:

$$\varepsilon = \frac{A}{c \cdot l}$$

Where:

- A is the absorbance.
- *I0* is the intensity of the monochromatic incident light (so before passing through the sample).
- *I* is the intensity of the monochromatic transmitted light (so after passing
- through the sample).

- ε is the molar extinction coefficient of the substance that causes the absorption of radiation.
- c is the concentration of the light-absorbing substance.
- *l* is the optical path length of the sample.

The Lambert-Beer law, a fundamental principle in spectrophotometric analysis, applies under specific conditions. First, the solution under analysis needs to be transparent and homogeneous, and the incident radiation needs to be monochromatic. Light scattering due to precipitates or suspended particles can produce unreliable results. Since very concentrated solutions may result in deviations due to increased light scattering or solute interactions, the law is more reliable for diluted solutions with absorbances that are not too high. The solute must also be stable at the measurement wavelength and maintain its chemical stability throughout the measurement process, not dissociating, combining, or decomposition. Significant light scattering or reflection from the solution should be avoided as this would ruin absorbance measurements. Lastly, the detector needs to exhibit a linear response to the intensity of the incident radiation in order to guarantee accurate light intensity measurements.If these conditions are respected, the Lambert-Beer law can be effectively used to calculate the concentration of an absorbing species in solution.

Specifically, the BioTek™ Synergy™ HTX Multi-Mode Microplate Reader was used to perform absorbance analyses on the Hard MIPs, with measurements taken between 250 nm and 500 nm at 1 nm intervals. For the Soft MIPs, absorbance measurements were carried out using the Shimadzu UV-2700i spectrophotometer, scanning from 200 nm to 400 nm with a resolution of 0.2 nm.

3.5.5. Calibration Curve

To properly interpret the results and quantify the concentrations of unknown samples, a calibration curve with known concentrations must be made for absorbance analyses. Additionally, this reduces the possibility of systematic and instrumental errors. The absorbance of several solutions at known concentrations must be measured in order to build the calibration curve, guaranteeing that all experimental parameters stay constant.

Additionally, it is important to calibrate the instrument by establishing a baseline, which is done by using a cuvette filled only with the solvent. In this study, the solvent used is demineralized

water, in which OTC is dissolved, and the characteristic absorbance peak is at 355 nm while for BSA is at 278 nm.

The absorbance at the chosen wavelength is plotted against the solution concentrations using the absorbance versus concentration method. An equation characterizing the connection between absorbance and concentration is derived through the use of linear regression.

The equation is:

$y = m \cdot x + b$

Where:

• y represents absorbance

• m is the slope (or extinction coefficient)

• x is the concentration

• b is the intercept.

The correlation coefficient, denoted as R, is an essential parameter that characterizes the equation's accuracy. The equation is a good approximation of the phenomenon's behavior if R is close to 1. The unknown concentration of the sample solutions can be determined using the calibration curve once it has been obtained.

4. Sample printing and Results Analysis

All the experiments related to Hard MIPs performed in this thesis followed a standardized workflow, consisting of the following steps:

1. Preparation of the formulation
2. Selection of CAD geometry
3. Optimization of the printing parameters and printing process
4. Post-curing of the samples
5. Removal of the template molecule
6. Rebinding process
7. Data analysis

For Soft MIPs, the workflow is similar but excludes the steps related to 3D printing and post-curing. The simplified procedure includes:

1. Preparation of the formulation
2. Polymerization of the samples
3. Removal of the template molecule
4. Data analysis

4.1. Formulation Preparation and Characterization for Hard MIP

The formulation used in this Thesis was already been characterized in previous studies, where both the NIP and MIP formulations exhibited viscosity values suitable for the DLP printing process. However, the MIP formulation demonstrated better performance during printing. In contrast, early studies found it challenging to print complex geometries using the NIP formulation. This didn't allow the direct comparison of MIP/NIP performances for complex three-dimensional shapes. Therefore, the first issue tackled in this work was to optimize NIP 3D printing.

4.1.1. Printing Parameters and Process Optimization

The selected geometry, known as 'gyroids', is a three-dimensional, complex, and undulating structure. It was chosen due to its high surface area and low volume, which makes it particularly suitable for maximizing antibiotic uptake. The printing parameters for the MIP formulation have already been optimized and are as follows:

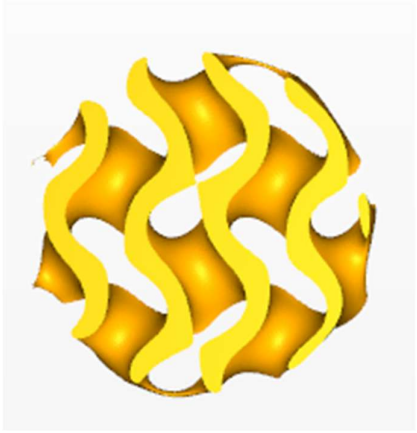

Figure 4.1 Gyroid geometry

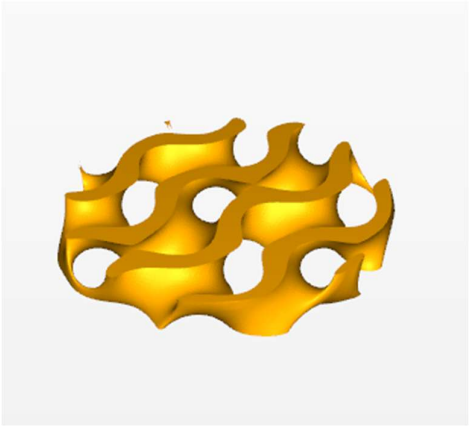

Figure 4.2 Gyroid geometry

GYROID MIP	Burn-in (0-200µM)	Range-1(200µM-1200µM)
Light intensity (mW/cm^2)	50	47
Exposure time (s)	32	35
Slice thickness (µM)	25	40

Subsequently, the printing parameters for printing this specific geometry using the NIP formulation are shown. To enable successful printing of this complex geometry, iit was necessary to incorporate a dye (methyl red) into the formulation. In fact, it is well-known that the presence of a dye can help to better control the extent of photopolymerization in 3D printing. [80]

The results obtained are visualized in Figures 4.3 and 4.4 . It is evident that NIP specimens were successfully 3D printed, enabling a more robust testing of hard MIP.

GYROID NIP	Burn-in (0-100µM)	Range-1(100µM-1200µM)
Light intensity (mW/cm^2)	20	20
Exposure time (s)	6	5
Slice thickness (µM)	15	40

Figure 4.3 Top view of a printed NIP. Image obtained with an optical microscope

Figure 4.4 Bottom view of a printed NIP. Image obtained with an optical microscope

4.1.2 Wettability

Since the uptake of target molecules from aqueous environment is the goal of MIPs, it is important to evaluate the wettability of the surfaces, measuring hydrophobicity/hydrophilicity. In this thesis, this was done measuring the water contact angle by depositing a single drop of water onto a flat surface specifically printed for this purpose. The measurements were performed on both MIP and NIP samples, before and after immersion in the washing solution. Based on the data obtained, it can be concluded that the surfaces are slightly hydrophilic (contact angle below 90°), and there are no significant differences between the MIP and NIP surfaces, nor between the samples before and after washing:

	Contact angle			**Average**	**Dev. standard**
NIP	71.1°	67°	62.5°	66.9°	3.51°
MIP	67.2°	58.6°	63	62.9°	3.51°
Washed NIP	60.9°	50.1°	61.8°	57.6°	5.32°
Washed MIP	64.7°	78.3°	60.2°	67.7°	7.69°

4.1.3 Debinding

The samples obtained through 3D printing undergo a post-processing phase that includes cleaning in ethanol to remove any unpolymerized resin, followed by post-curing in a UV chamber to enhance the structural integrity of the printed material. Once these steps are completed, the samples are ready for the template extraction process.

The washing procedure used is the one described in the previous chapter. It is important to replace the washing solution once it becomes saturated with the template molecule, in this case, oxytetracycline (OTC). If the solution is not changed regularly, the OTC can be reabsorbed by the sample rather than being effectively removed. The efficiency of the washing step can be macroscopically observed by a change of color in the specimens (figures 4.5 and 4.6), however the complete removal of OTC is confirmed when the absorbance spectrum no longer shows its characteristic peak at 355 nm (figure 4.7). This washing procedure is time-consuming and requires the continuous presence of an operator to monitor and analyze the washing solutions at regular intervals.

Figure 4.5 MIP before debinding

Figure 4.6 MIP after debinding

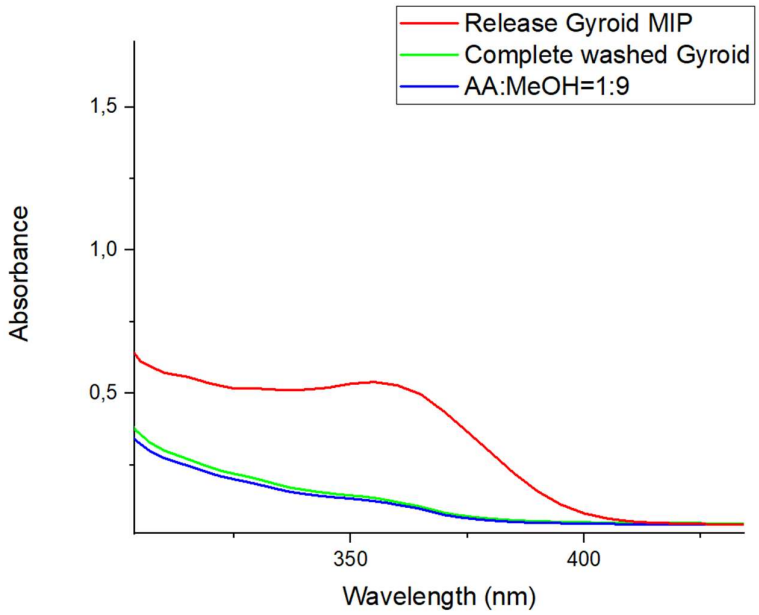

Figure 4.7 Absorbance spectra of release of gyroid MIP

4.2. Rebinding experiments

4.2.1. OTC calibration curve

Building the OTC calibration curve was the first stage in the rebinding experiments. A range of solutions with different molarities (200, 150, 125, 100, 75, 50, 25, 10, and 1) µM were made in order to accomplish this. Making the stock solution, which involved dissolving 11 mg of OTC in 15 mL of demineralized water, was the first step in the procedure. This stock was then diluted to create the remaining solutions.

A plate reader was used to measure the absorbance of each solution, using deionized water (H_2O) as the blank. At a wavelength of 355 nm, absorbance values were measured for concentrations ranging from 200 µM to 0 µM (blank solution). The graph displayed in Figure 4.8 was produced by plotting these data points.

The calibration curve, which is represented by the following equation, is the consequent linear relationship between absorbance and known concentrations: $y = 0.0075x + 0.013$

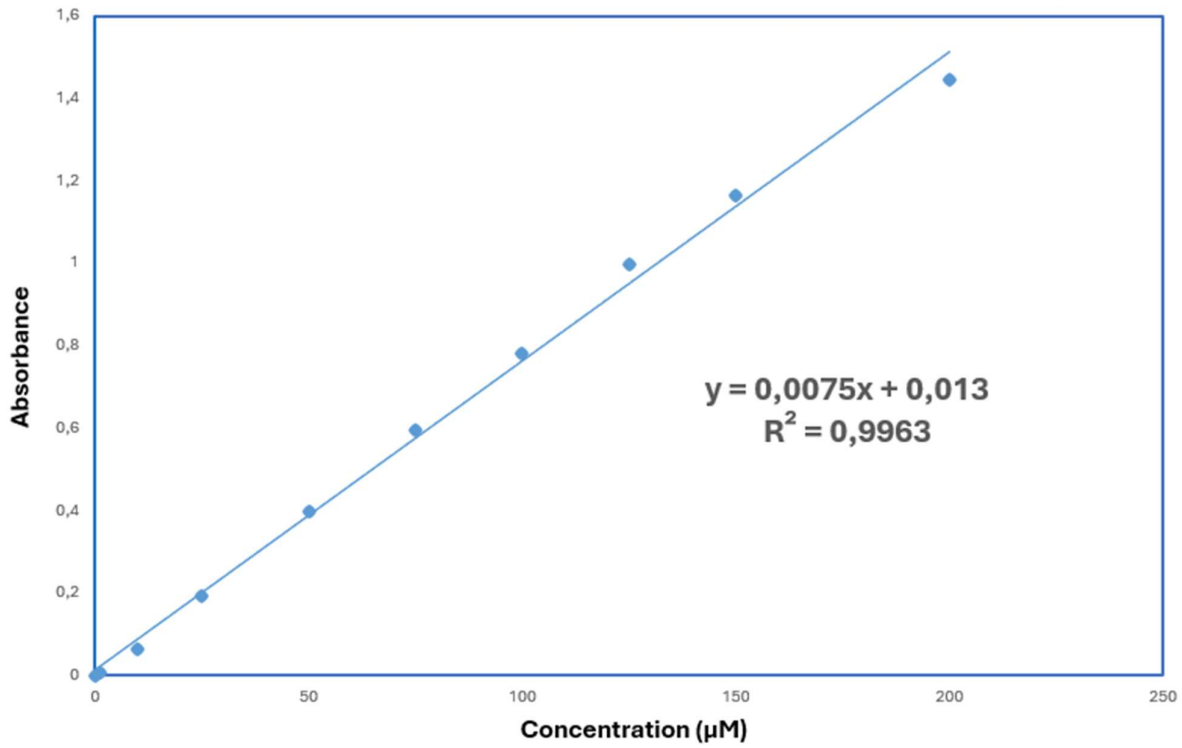

Figure 4.8 Calibration Curve

The correlation coefficient (R^2) was determined in order to assess the calibration curve's accuracy. With values ranging from 0 to 1, R^2 measures the degree of correlation between the fitted regression line and the observed data points. A better fit is indicated by higher R^2 values. The R^2 value of 0.9963 in this instance indicates a very good fit.

Once the calibration curve and its equation are established, the measured absorbance values of unknown samples can be used to calculate the concentration of OTC in those samples.

4.2.2. Experimental Series, GYROIDS1: MIP and NIP

The rebinding experiment was carried out using triplicate samples of MIP and NIP. The samples were incubated in a 100 µM OTC solution following template removal treatment. They were placed on an oscillating plate to guarantee uniform mixing during the set incubation period, which was held at 26°C. In order to get accurate results, the same conditions were used to incubate an additional control sample that contained only OTC and neither MIP nor NIP. Three time points (3h, 5h, and 7 h) were used to record absorbance spectra.

At each time step the absorbance spectra were compared to the solution that contained only OTC, the MIP samples displayed a weaker signal, indicating that the MIPs were able to capture

a portion of the target molecule, the antibiotic. Although the NIPs lack of cavities that specifically match the shape of the target molecule, a decrease in the signal was still observed, likely due to nonspecific binding interactions. At 3 hours the Figure 4.9 shows a significantly greater decrease in the absorbance spectra for the MIP samples, indicating a faster uptake of OTC due to the presence of specific binding cavities. However, at 5 and 7 hours (Figures 4.10 4.11), the difference between MIP and NIP becomes less pronounced.

For statistical analysis, the percentage removal was selected as the key parameter. This measure compares the antibiotic concentration at a given time point in the presence of MIP or NIP to the concentration of the control containing only OTC. The percentage removal provides a numerical representation of the amount of the antibiotic molecules captured by the samples. From the resulting graph (Figure 4.12), it is clear that the MIPs exhibit superior performance compared to the NIPs in capturing the antibiotic.

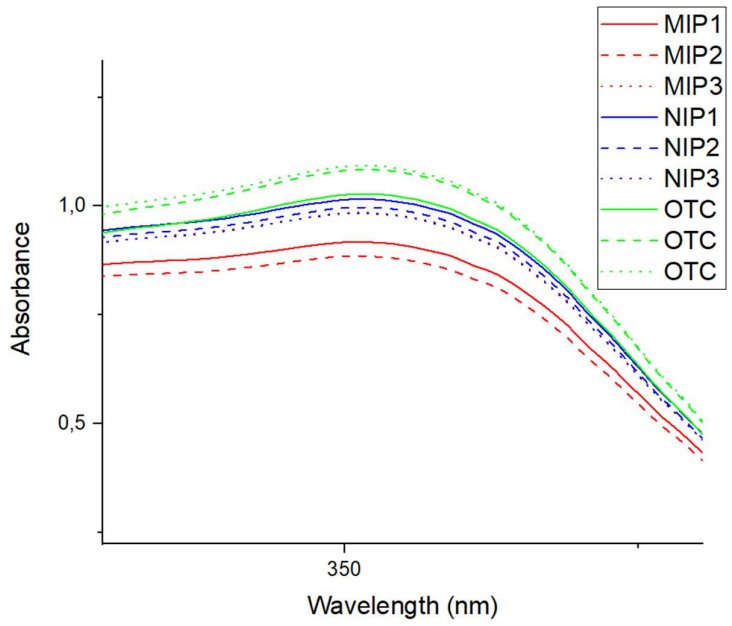

Figure 4.9 Absorption spectra of 3 MIPs and 3 NIPs incubated in rebinding solution 100 µM after 3h

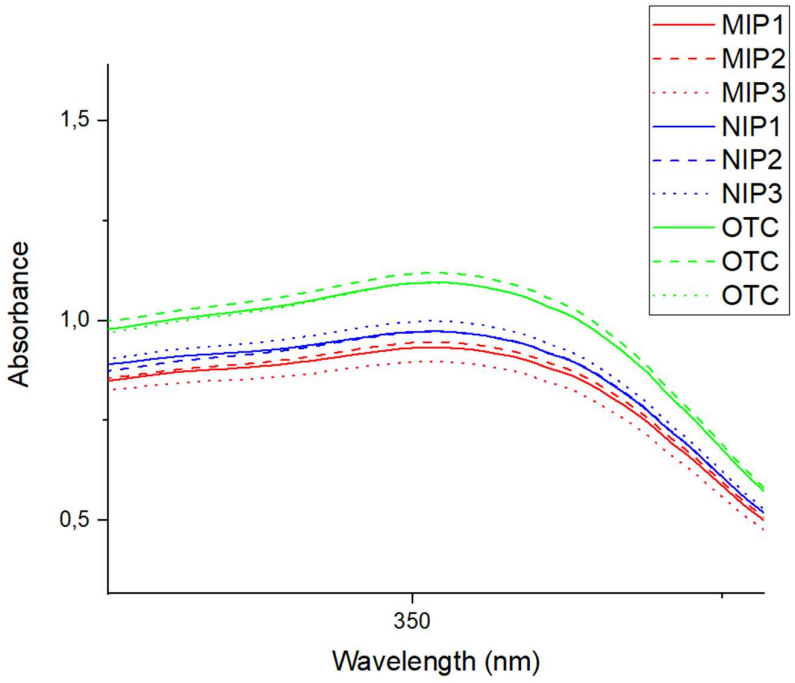

Figure 4.10 Absorption spectra of 3 MIPs and 3 NIPs incubated in rebinding solution 100 µM after 5h

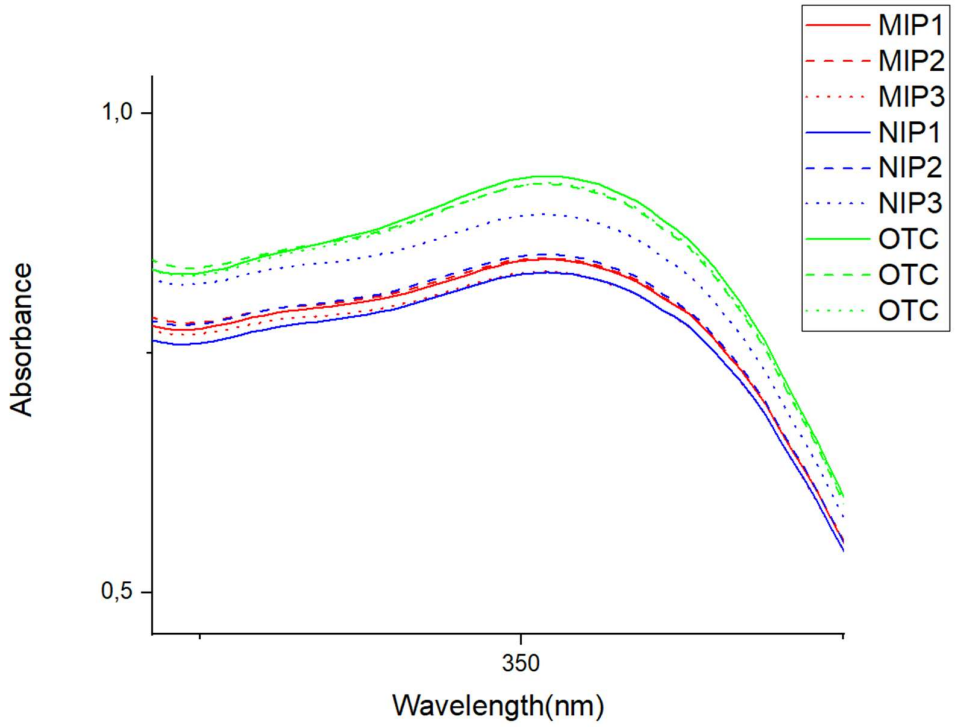

Figure 4.11 Absorption spectra of 3 MIPs and 3 NIPs incubated in rebinding solution 100 µm after 7h

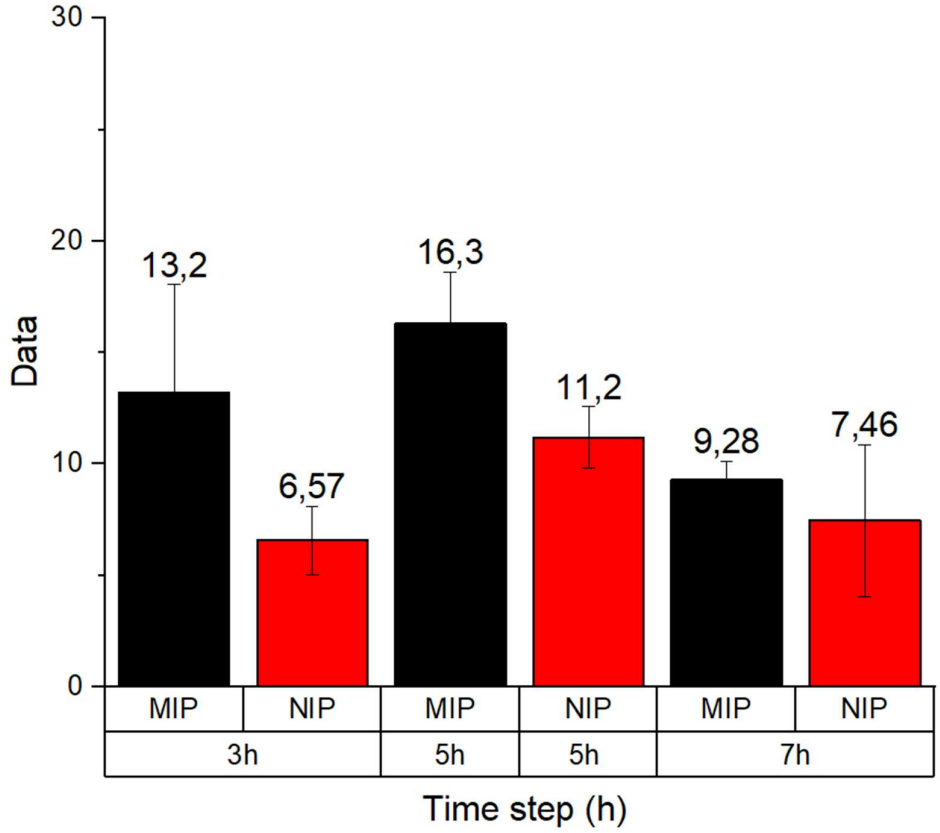

Figure 4.12 Percentage Removal of 3 MIPs and 3 NIPs

4.2.3. Second experiment, GYROIDS2: MIP and NIP

The next experiment was conducted using triplicate samples for each time point, with measurements taken simultaneously at the designated intervals. The experiment was set up so that three distinct trials were started at various times, allowing all results to be obtained within the same experimental period, in order to guarantee consistency and reduce errors related to the measuring apparatus. Data collection time points were extended to 3, 5, and 24 hours, and the solution containing only OTC was incubated at a concentration of 100 µM.

The MIPs effectively absorbed the target template, as evidenced by the lower signal in the absorbance spectra of the MIP samples when compared to the control solution that contained only OTC (Figures 4.13, 4.14 and 4.15) Although the NIP samples' absorbance decreased as a result of nonspecific binding, their signal was noticeably stronger than the MIPs, indicating that the NIPs were less effective at capturing the antibiotic. As expected, the percentage removal

analysis showed in Figure 4.16 confirms the MIPs superior performance over the NIPs and their increased capacity to efficiently capture the target molecule.

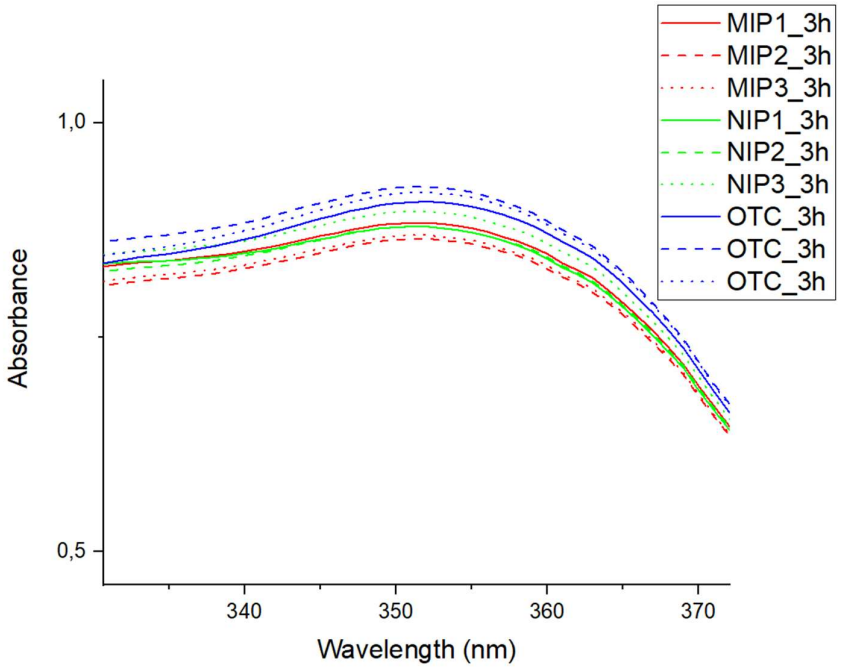

Figure 4.13 Absorption spectra of 3 MIPs and 3 NIPs incubated in rebinding solution 100 µM after 3h

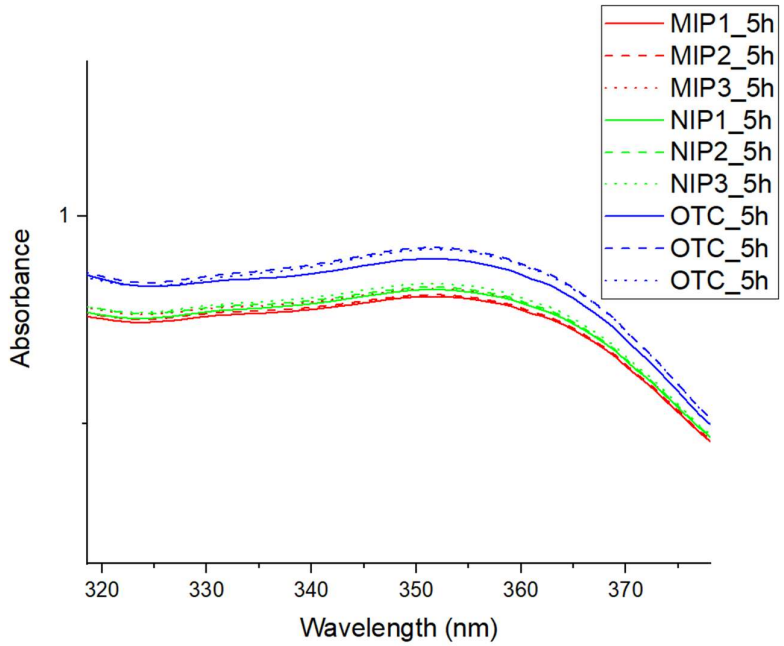

Figure 4.14 Absorption spectra of 3 MIPs and 3 NIPs incubated in rebinding solution 100 µM after 5h

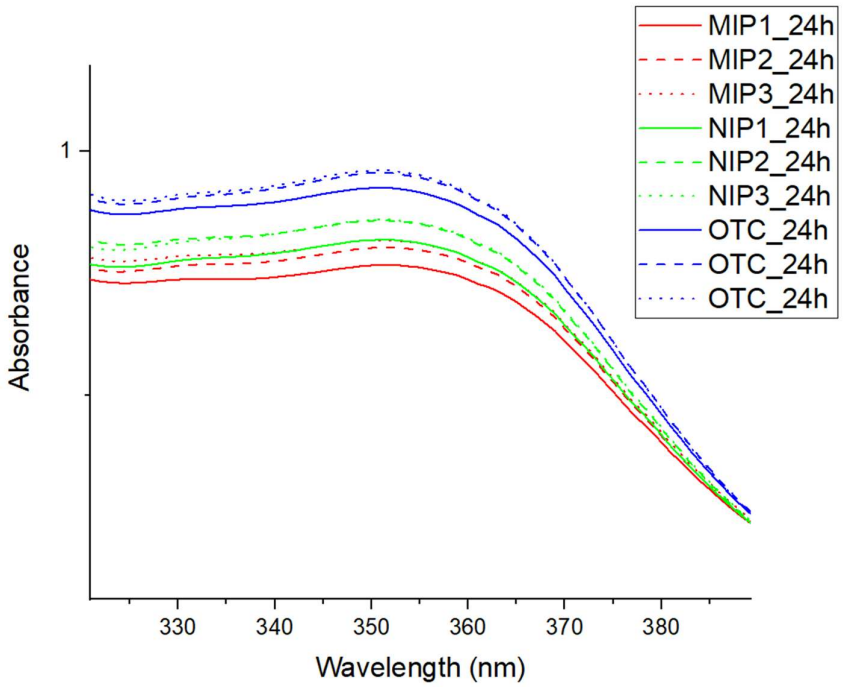

Figure 4.15 Absorption spectra of 3 MIPs and 3 NIPs incubated in rebinding solution 100 µM after 24h

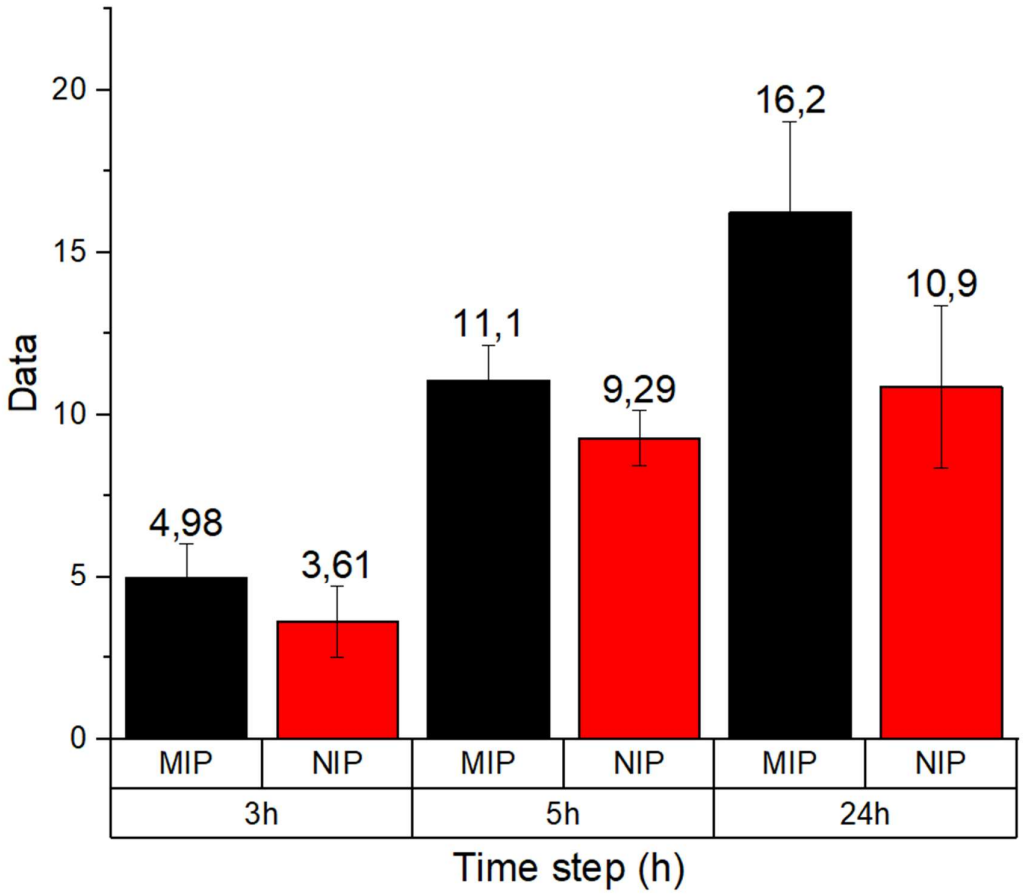

Figure 4.16 Percentage Removal of 3 MIPs and 3 NIPs

In summary, the work presented in this thesis led to the successful synthesis of gyroid-structured NIPs, which made it possible to perform a direct comparison with their MIPs counterparts. Based on the experimental data, the MIPs consistently demonstrated enhanced selectivity and binding efficiency relative to the NIPs, confirming their superior performance. These findings highlight the effectiveness of molecular imprinting in producing polymers with tailored recognition sites and suggest strong potential for the application of MIPs in areas such as sensing, separation, and targeted delivery.

4.3. Formulation Preparation and Characterization for Soft MIP

The formulation of soft MIPs containing BSA was obtained following the procedure described in the previous chapter. BSA was first dissolved in deionized water using magnetic stirring, followed by the addition of the other components. The final resin obtained appears as shown in Figure 4.17. This formulation is based on a study conducted by Ran D. et al. [81], but it was modified to make it suitable for the printing process by changing the crosslinker and adding a photoinitiator.

To determine the optimal amount of deionized water required to dissolve the resin components, various concentrations (20%, 40%, 60%, and 80% relative to the other compounds) were tested. As shown in Figure 4.18, only the formulations with 20% and 80% of deionized water resulted trasparent whereas the others formed cloudy emulsions. Ultimately, the formulation containing 20% deionized water was selected as the final one, as the 80% formulation was not suitable for photopolymerization.

Figure 4.17 Mip formulation containing BSA

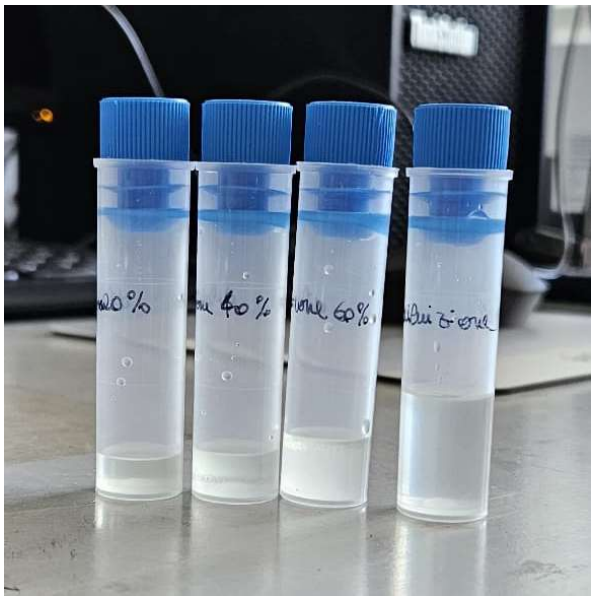

Figure 4.18 Resin formulation with different ratio of deionized water

4.3.1. Formulation Characterization

RHEOLOGY

As described in the previous chapter, rheological tests were performed to evaluate the viscosity profiles of the MIP and NIP formulations. The results of these measurements are presented in the following Figures 4.19 and 4.20 . It is important to note that the NIP formulation exhibited a phenomenon of rapid gel formation as water evaporates, not allowing testing due to modification of properties. To mitigate this, silicone oil was applied around the edge of the rheometer plate to prevent crystallization during the test. The same procedure was adopted during the measurement of the MIP formulation to maintain consistency.

From the graph in Figure 4.19, it is evident that at low shear rates, the viscosity of the MIP formulation is significantly higher than that of the NIP formulation. As the shear rate increases, the MIP formulation exhibits shear-thinning behavior, characterized by a progressive decrease in viscosity with increasing shear rate. The NIP formulation displays a more stable viscosity profile across the tested shear rates, indicating less pronounced structural changes under shear. This contrast suggests that the presence of the protein in the MIP formulation strongly

influences its rheological behavior. At higher shear rates, both formulations tend to converge toward lower viscosity values.

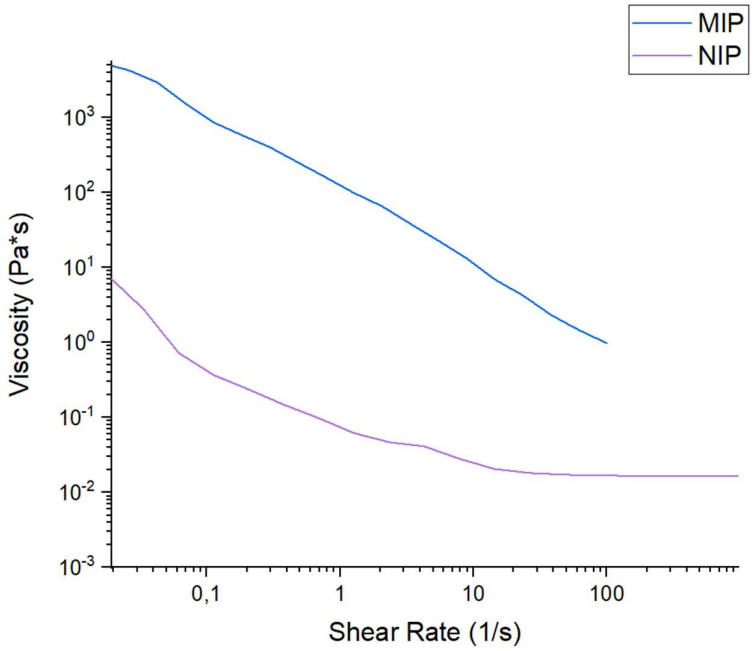

Figure 4.19 Viscosity of MIP and NIP formulations under continuous shear rate sweep

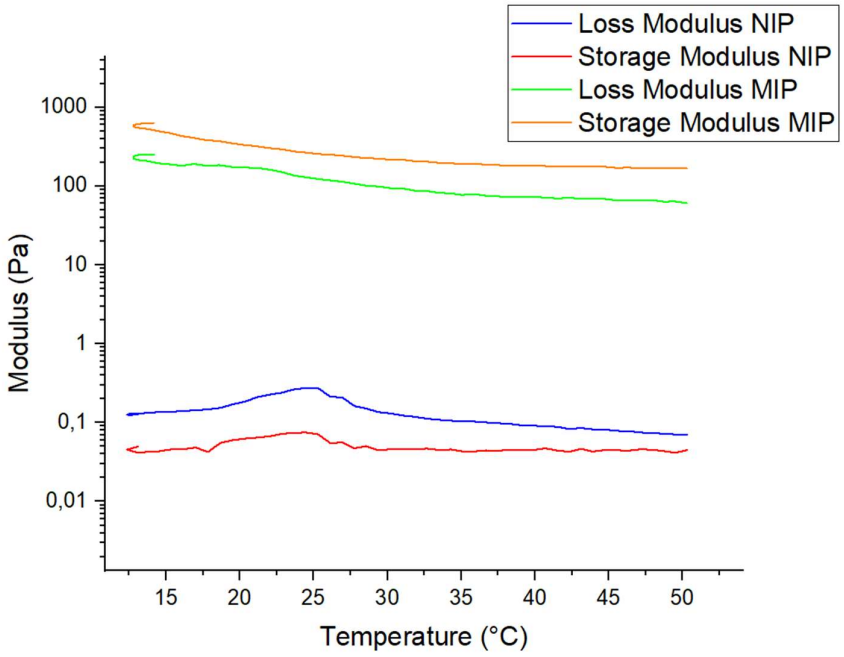

Figure 4.20 Storage and Loss Modulus in function of the temperature

The Figure 4.20 illustrates the temperature-dependent viscoelastic behavior of both MIP and NIP formulations. The results indicate that the NIP formulation exhibits a greater sensitivity to temperature in the range of 18 °C to 30 °C. This behavior may be attributed to the presence of N-isopropylacrylamide (NIPAM), a thermoresponsive polymer known to have a lower critical solution temperature (LCST) at approximately 32 °C. [82] In contrast, the MIP formulation demonstrated consistently higher values of both the storage modulus (G') and the loss modulus (G") compared to the NIP formulation across the entire temperature range. This again is consistent with the increased viscosity induced by the presence of BSA-A general decrease in the viscoelastic modulus was observed at elevated temperatures, indicating a softening of the material structure with temperature.

PHOTO RHEOLOGY

Subsequently, a photorheological test was conducted to analyze the behavior of the storage modulus (G') over time.

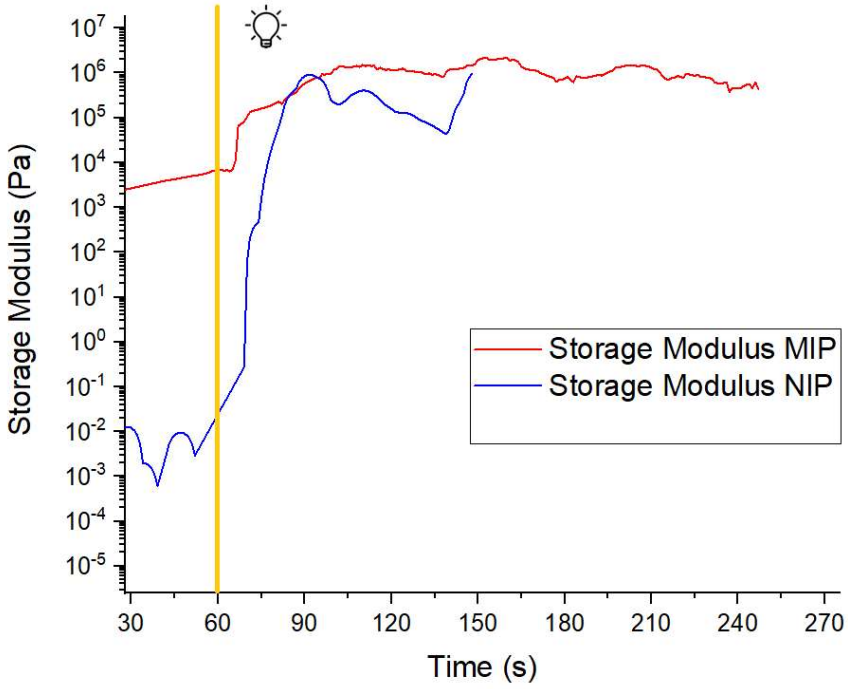

Figure 4.21 Real-time photorheological measure of the MIP and NIP formulations

As expected initially, the NIP formulation exhibits very low storage modulus (G') values, consistent with its highly liquid nature, whereas the MIP formulation displays higher G' values. At the 60-second mark, the UV light source is activated, and the graph shown in Figure 4.21

reveals a steep increase in the G' modulus for both formulations, signifying the onset of photopolymerization and the transition from liquid to solid state after almost 2 minutes.

The differences observed in the rate of increase and the final magnitude of G' between the MIP and NIP formulations can be attributed to their distinct molecular architectures and compositions. The MIP formulation demonstrates a sharp and rapid rise in storage modulus, reaching its maximum value relatively within approximately 5 seconds, which suggests a fast and efficient photopolymerization process. In contrast, the NIP formulation shows a delayed increase in G', which is likely due to its highly liquid nature. This formulation requires a longer time, nearly 20 seconds, to initiate and complete the polymerization process.

Having measured the possibility to form photocurable specimens, those were fabricated to test the capabilities of those formulations as MIP.

4.3.2. BSA calibration curve

As the first step to evaluate BSA release, the calibration curve was obtained. A range of solutions with different molarities (90, 60, 45, 30, 15, 9, 3 μM) were made. For the stock solution 239,15 mg of BSA were dissolved in 30 mL of deionized water. This stock was then diluted to create the remaining solutions.

A plate reader was used to measure the absorbance of each solution, using deionized water (H2O) as the blank. At a wavelength of 278 nm, absorbance values were measured for concentrations ranging from 90 μM to 0 μM (blank solution). In Figure 4.22 is displayed the graph obtained by plotting these data points.

The calibration curve is represented by the following equation and is the consequent linear relationship between absorbance and known concentrations:

$y = 0.00371x + 0.0131$

The correlation coefficient (R^2) has a value of 0.9983 and it indicates a very good fit between the fitted regression line and the observed data points. Once the calibration curve and its equation are established, the measured absorbance values of unknown samples can be used to calculate the concentration of BSA in those samples.

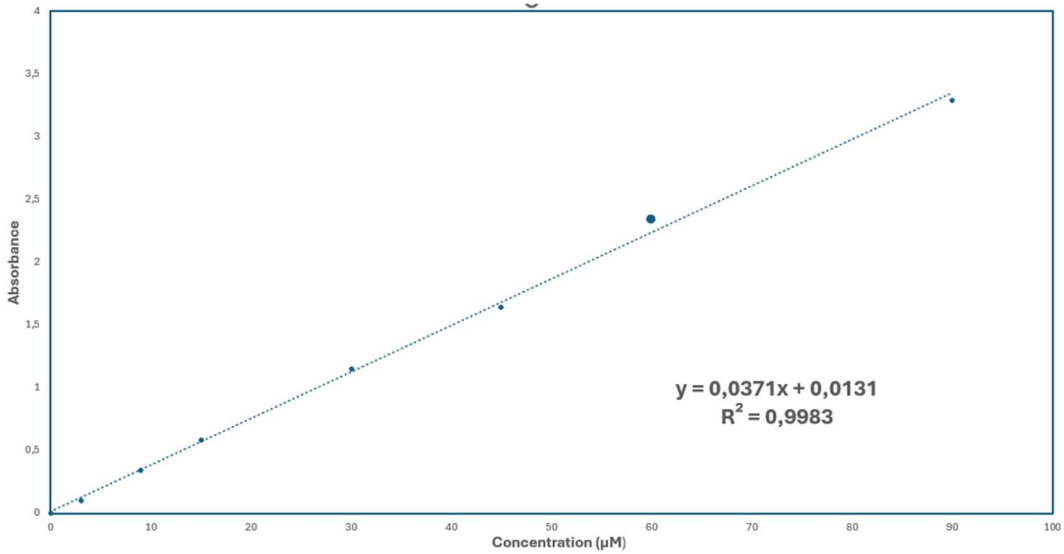

Figure 4.22 Calibration Curve

4.3.3 Debinding for Soft MIPs

As already introduced, after polymerization the removal of target molecule is in the first step to follow. In the case of Soft MIPs, the washing procedure was similar to the one used for Hard MIPs; the only difference was the washing solution employed. In this case, the washing solution consisted of deionized water (H_2O) supplemented with sodium chloride (NaCl) at a concentration of 100 mmol/L To confirm that the MIPs were releasing the target molecule, in this case, a protein, the release from both MIP and NIP samples was measured after only 4 h. However, the absorbance spectra did not show the characteristic protein peak at 278 nm, as expected. As shown in Figures 4.23 and 4.24, the spectra of the MIP and NIP releases were nearly identical.

Subsequent measurements were also taken after 7 h and 72 h, yet none displayed the expected characteristic peak. This suggests that either the washing procedure was not properly optimized or that the protein may have been denatured during the polymerization process. To investigate this further, additional measures were conducted.

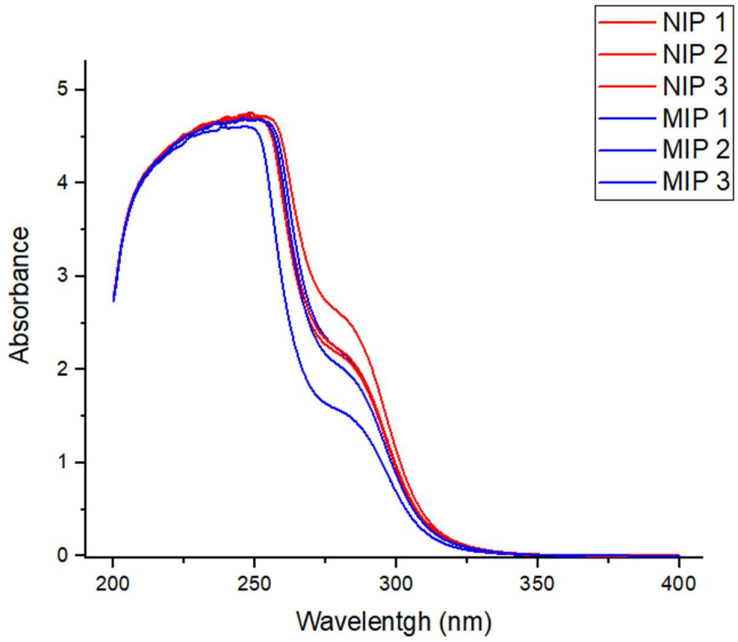

Figure 4.23 3 MIP and 3 NIP Release in H_2O and NaCl after 4h

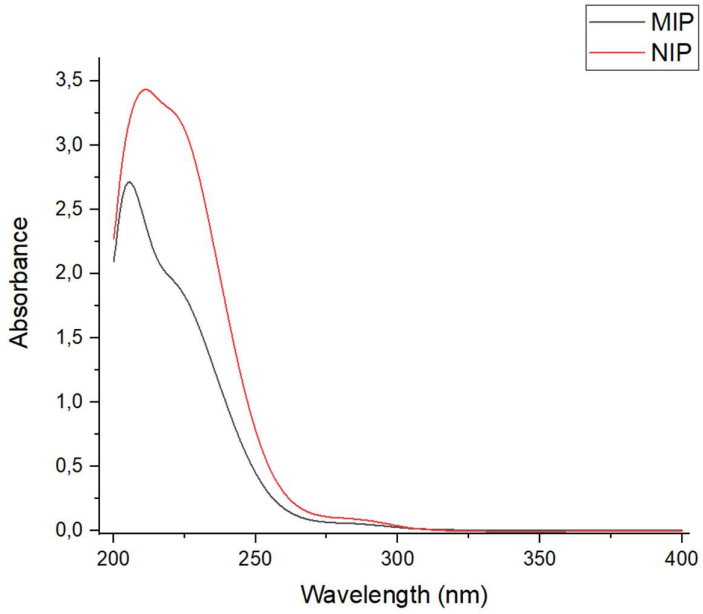

Figure 4.24 MIP and NIP Release in H_2O and NaCl after 72h

4.3.4 Key Issue in Soft MIPs characterization

As previously mentioned, the debinding procedure suggested that the protein might have been denatured, and additional measurements were conducted to determine why this occurred. Protein denaturation could have taken place at three different stages: during the initial preparation of the mixture, where the protein (BSA) is dissolved in water with the aid of magnetic stirring, during the addition of functional monomers, crosslinker, and photoinitiator, or during UV exposure of the final resin.

To investigate this, BSA was individually mixed with each component of the formulation. The absorbance spectra revealed that the characteristic protein peak was absent when BSA was combined with NIPAM, indicating that NIPAM could be responsible for denaturing the protein.

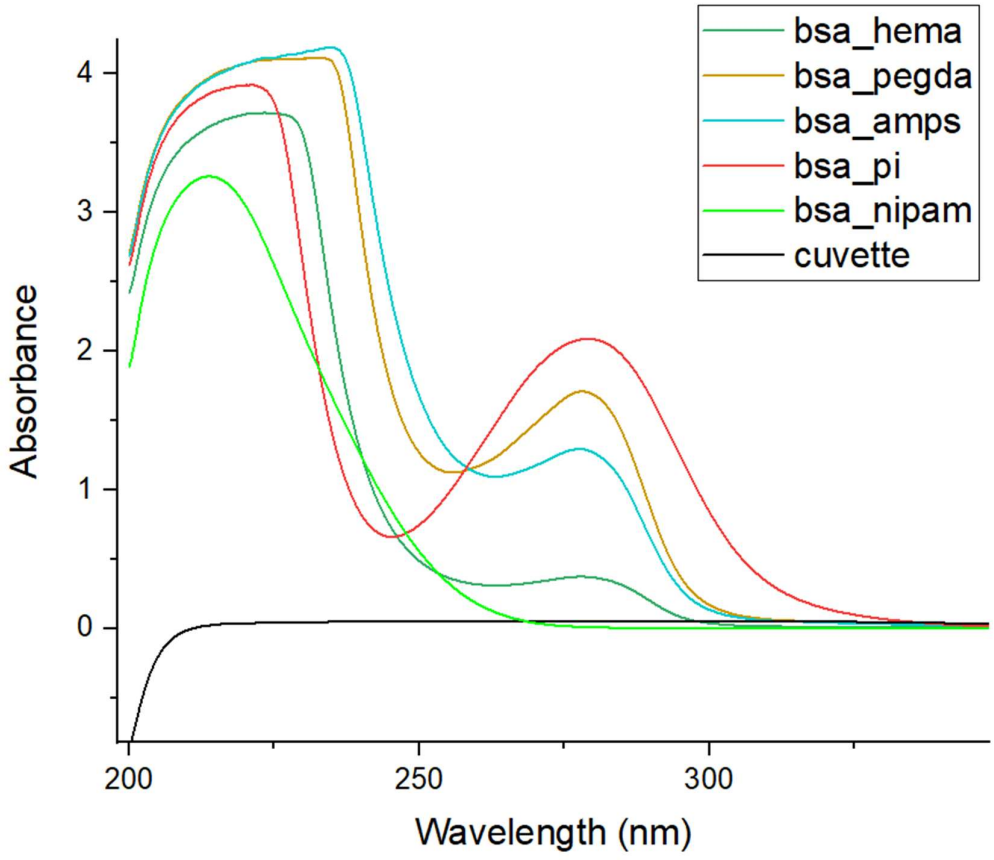

Figure 4.25 Absorbance of each component mixed with BSA

Following this, a study was conducted to determine the optimal ratio between NIPAM and BSA. Several formulations were prepared, each containing increasing amounts of NIPAM relative to a constant BSA concentration. 166 mg of BSA dissolved in 5 ml of deionized water and then (16, 32, 64, 128, 166, 332) mg of NIPAM were added. The absorbance spectra of these formulations in Figure 4.26 were analyzed, and it was observed that when the concentration of NIPAM reached 38.5% relative to BSA, the characteristic protein peak disappeared. The missing peak could be attributed to either the denaturation of BSA or the possibility that NIPAM's absorbance spectrum overlaps with that of BSA, masking its signal.

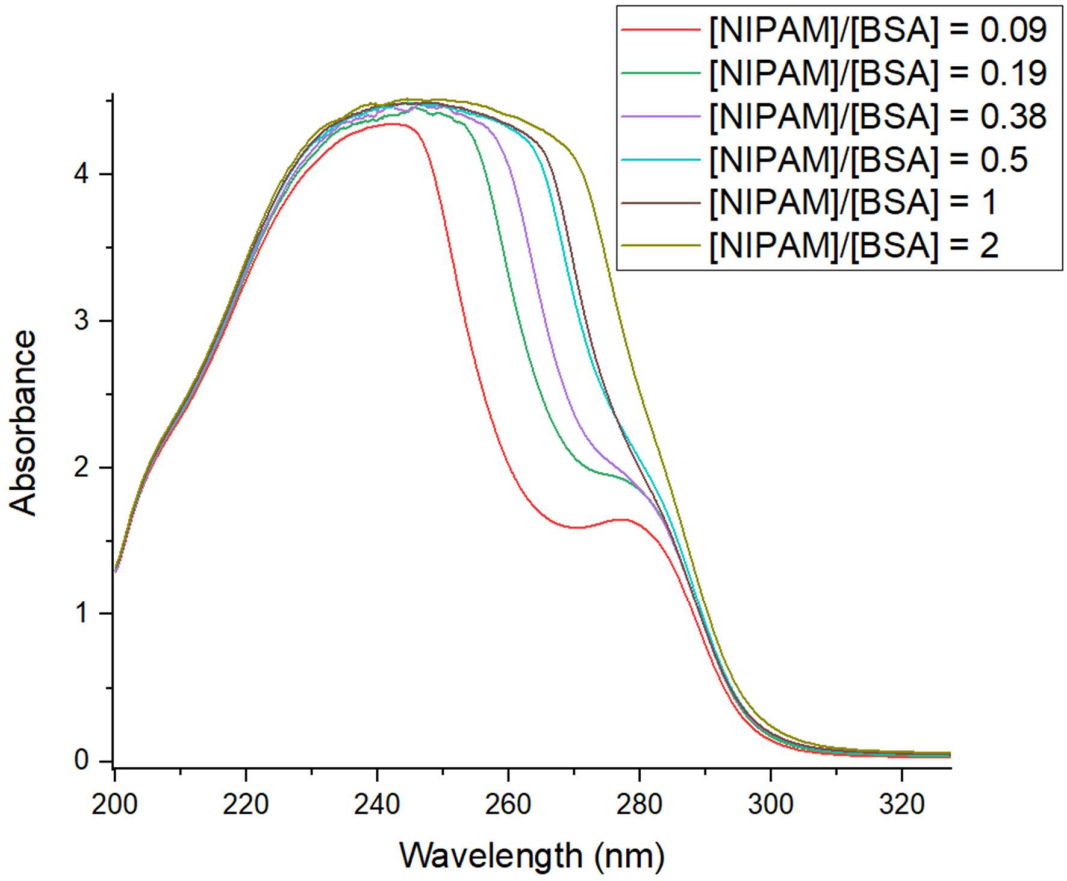

Figure 4.26 Absorbance of different ratio of NIPAM and BSA

Subsequently, to verify this hypothesis, an additional measurement was carried out with 332 mg of NIPAM dissolved in 5 mL of deionized water. The absorbance spectrum obtained, as presented in Figure 4.27, shows a partially overlap with the BSA spectrum. This represents a bottleneck in the development of MIP and the results are in contrast with the results reported in the reference literature.

Therefore these preliminary testing highlights the necessity of starting with a new formulation for the development of soft MIPs.

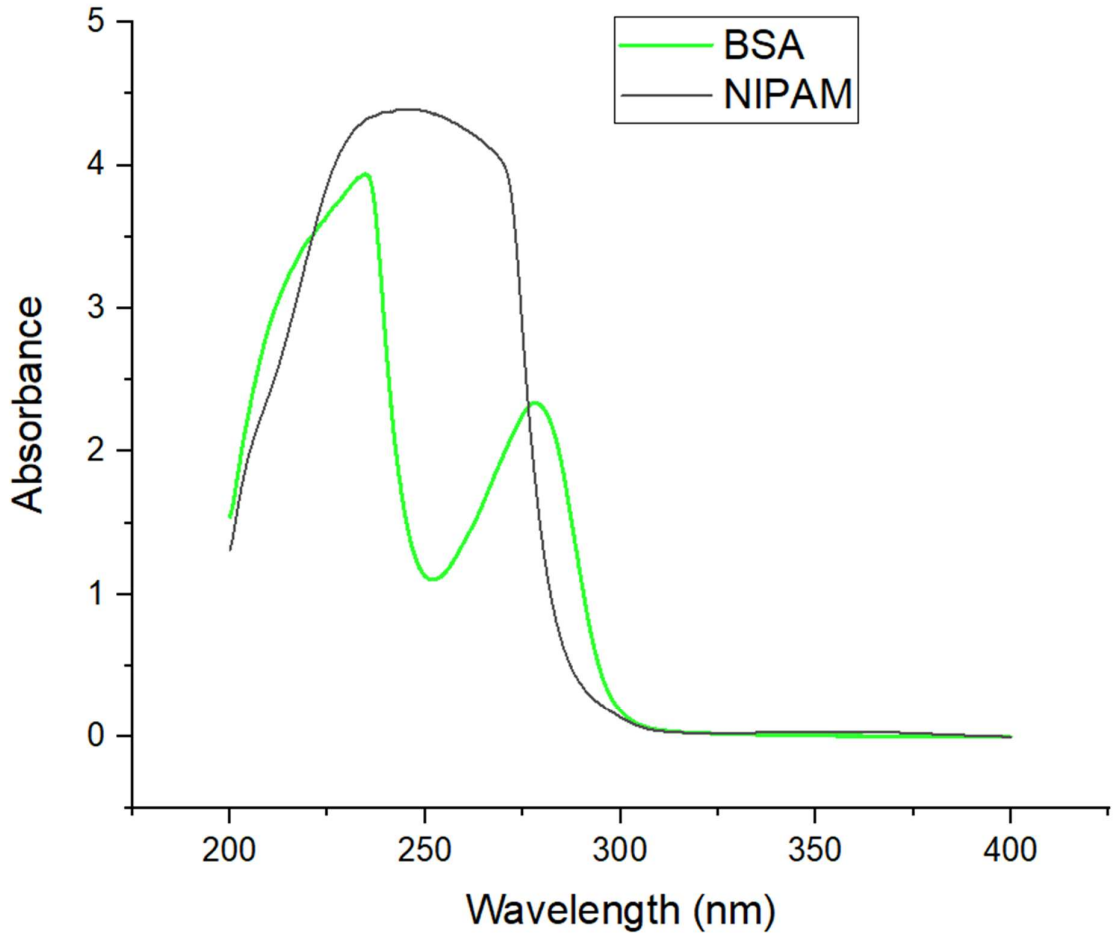

Figure 4.27 Comparison between BSA spectra and NIPAM

5. Conclusions and future work

This work aimed to fabricate two different types of Molecularly Imprinted Polymers (MIPs): Hard and Soft. MIPs are synthetic receptors that mimic the natural molecular recognition mechanism of biological receptor molecules. These materials are capable of selectively detecting target molecules that have been previously imprinted into their structure.

In the first case, Hard MIPs were fabricated using Digital Light Processing (DLP) 3D printing. The NIP formulation was optimized to enable accurate printing of the desired geometry, allowing a direct comparison between the performance of MIPs and NIPs. Following fabrication, the ability of the materials to rebind the target molecule used during the imprinting process was assessed using the batch rebinding method and analyzed via UV-Vis spectroscopy. The results demonstrated promising performance, with MIPs exhibiting a higher binding affinity compared to NIPs. However, issues with experimental repeatability were encountered and should be addressed in future studies. Additionally, future work could focus on evaluating the selectivity of the MIPs by testing their rebinding behavior in solutions containing different target molecules. Such studies would help confirm that the MIPs preferentially rebind the imprinted molecule over those forming non-specific interactions.

In the second case, the selected target molecule was a protein, larger and more challenging to imprint. In this context, a reference formulation reported in literature was used as starting point. The formulation incorporating BSA shows increased viscosity but demonstrated to be suitable for photopolymerization. However, testing the MIPs efficiency, significant difficulties were encountered due to the risk of protein denaturation. It was found that the concentration of N-isopropylacrylamide (NIPAM) may interfere with protein activity. With this insight, future research should aim to optimize the ratio between functional monomers and the protein to minimize denaturation. Moreover, efforts should be directed toward improving the printability of the resulting resin to enable the successful application of 3D printing techniques and the production of high-quality MIP samples.

Bibliography

[1] S. kgönüllü, S. Kılıç, C. Esen e A. Denizli, «Molecularly Imprinted Polymer-Based Sensors for Protein Detection,» *Polymers,* pp. 15, 629, 2023. doi:10.1016/j.bios.2023.115774

[2] C. A. e. al., «Molecular imprinting science and technology: A survey of the literature,» 2006. doi:10.1002/jmr.760

[3] L. D. a. W. H. C. Alexander, «Imprinted polymers: Artificial molecular recognition materials with applications in synthesis and catalysis,» *Elsevier Ltd.,* 2003. doi:10.1016/S0040-4020(03)00152-2

[4] M. G. S. A. H. S. M. M. Sonia Bahrani, «Chapter 11 - Applications of molecularly imprinted polymers,» *Interface Science and Technology,* vol. Volume 33, pp. 655-699,2021. doi:10.1016/B978-0-12-818805-7.00002-3

[5] M. E. Byrne, K. Park e N. A. Peppas, «Molecular imprinting within hydrogels.,» p. 149–161, 2002. doi:10.1016/s0169-409x(01)00246-0

[6] G. Wulff, «Molecular imprinting in cross-linked materials with the aid of molecular templates- a way towards artificial antibodies,» *Angewandte Chemie International Edition in English,* vol. 34, n. 17, pp. 1812-1832, 1995. doi:10.1002/anie.199518121

[7] K. R. O. Mosbach, «The Emerging Technique of Molecular Imprinting and Its Future Impact on Biotechnology,» *Nat Biotechnol,* vol. 14, p. 163–170, 1996. doi:10.1038/nbt0296-163

[8] P. N. Vandita Kakkar, «Role of molecularly imprinted hydrogels in drug delivery - A current perspective,» *International Journal of Pharmaceutics,* vol. 625, 2022. doi:10.1016/j.ijpharm.2022.121883

[9] M. W. a. J. Datta, «Synthesis and polymerisation techniques of molecularly imprinted,» *Comprehensive Analytical Chemistry,* vol. 86, 2019. doi:10.1016/bs.coac.2019.05.011

[10] X. S. L. J. Chen L, «Recent advances in molecular imprinting technology: current status, challenges and highlighted applications,» *Chem Soc Rev,* 2011. doi:10.3390/ijms12074327

[11] «Principio Le chatelier,» [Online]. Available: https://www.chimica-online.it/download/principio-le-chatelier.htm. [Accessed 13 July 2025].

[12] J. D. Marty, «Molecular Imprinting: State of the Art and Perspectives,» *Advances in Polymer Science,* 2005. doi:10.1007/b97573

[13] M. Włoch, «Synthesis and polymerisation techniques of molecularly imprinted polymers,» 2019. doi:10.1016/bs.coac.2019.05.011

[14] A. Speltini, A. Scalabrini, F. Maraschi, M. Sturini e A. Profumo, «Newest applications of molecularly imprinted polymers for extraction of contaminants from environmental and food matrices: A review,» *Analytica Chimica Acta,* 2017. doi:10.1016/j.aca.2017.04.042

[15] L. T. S. G. A. V. S. A. a. T. J. G. C. C. Villa, «Molecularly imprinted polymers for food applications: A review,» 2021. doi:10.1016/j.tifs.2021.03.003

[16] B. M. T Sajini, «A brief overview of molecularly imprinted polymers: Highlighting computational design, nano and photo-responsive imprinting,» *Talanta Open,* vol. 4, 2021. doi:10.1016/j.talo.2021.100072

[17] G. V. e. al, «Molecularly imprinted polymers: Present and future prospective,» 2011. doi: 10.3390/ijms12095908

[18] A. M. C. C. A.-L. a. A. C. Rosa A. Lorenzo, «To Remove or Not to Remove? The Challenge of Extracting the Template to Make the Cavities Available in Molecularly Imprinted Polymers (MIPs),» vol. 12, n. 7, pp. 4327-4347, 2011. doi:10.3390/ijms12074327

[19] K. J. S. D. Y. S. G. J. Shea, «Fluorescence probes for evaluating chain solvation in network polymers. An analysis of the solvatochromic shift of the dansyl probe in macroporous styrene-divinylbenzene and styrene-diisopropenylbenzene copolymers,» *Macromolecules,* pp. 1722-1730, 1989. doi:10.1021/ma00194a037

[20] M. W. T. C. C. L. S.H Ou, «Polyacrylamide gels with electrostatic functional groups for the molecular imprinting of lysozyme,» *Analytica Chimica Acta,* vol. 504, n. 1, pp. 163-166, 2004. doi:10.1016/S0003-2670(03)00531-2

[21] L. S. S. Levi, «Simulation of Protein-Imprinted Polymers. 1. Imprinted Pore Properties,» *The Journal of Physical Chemistry B,* 2010. doi:10.1021/jp9087767

[22] B. C. B. S. C. C. K. L. O. P. E. K. C. P. S. D. S. B. Ellwanger A, «Evaluation of methods aimed at complete removal of template from molecularly imprinted polymers.,» vol. 126, n. 6, 2001. doi:10.1039/b009693h

[23] H. Y. J. Z. Guo-Qi Fu, «Imprinting effect of protein-imprinted polymers composed of chitosan and polyacrylamide: A re-examination,» *Biomaterials,* vol. 29, n. 13, 2008. doi: 10.1016/j.biomaterials.2008.01.019

[24] A. Hillberg, K. Brain e C. Allender, «Design and evaluation of thin and flexible theophylline imprinted polymer membrane materials,» vol. 22, p. 223–231, 2009. doi:10.1002/jmr.935

[25] J. E. D. K. F. H. A. M. M. S. D. W. T. G. V. K. B.E. Richter, «Extraction of polychlorinated dibenzo-p-dioxins and polychlorinated dibenzofurans from environmental samples using accelerated solvent extraction (ASE),» *Chemosphere,* vol. 34, n. 5-7, 1997. doi: 10.1021/ac00226a017

[26] C. A. Alvarez-Lorenzo, Handbook of Molecularly Imprinted Polymers, Smithers Rapra Publishing, 2013. "https://books.google.it/books?id=Ma3OngEACAAJ"

[27] L. d. C. M. Luque-García JL, «Focused microwave-assisted Soxhlet extraction: devices and applications,» vol. 64, n. 3, pp. 571-7, 2004. doi:10.1016/j.talanta.2004.03.054.

[28] S.-B. C. A. B. G.-V. A. Tadeo JL, «Application of ultrasound-assisted extraction to the determination of contaminants in food and soil samples,» vol. 1217, n. 16, pp. 2415-40, 2010. doi:10.1016/j.chroma.2009.11.066

[29] B.-G. E. S.-M. A. Fidalgo-Used N, «Sample handling strategies for the determination of persistent trace organic contaminants from biota samples,» *Anal Chim Acta,* 2007. doi:10.1016/j.aca.2007.03.004

[30] A. C. E. I. Miguel Herrero, «Sub- and supercritical fluid extraction of functional ingredients from different natural sources: Plants, food-by-products, algae and microalgae: A review,» *Food Chemistry,* vol. 98, n. 1, 2006. doi:10.1016/j.foodchem.2005.05.058

[31] M. V. D. C. S. K. A. A. Lamaoui A, «Molecularly imprinted polymers: A closer look at the template removal and analyte binding.,» *Biosens Bioelectron,* 2023. doi:10.1016/j.bios.2023.115774

[32] K. H. R. Hongyuan Yan, «Characteristic and Synthetic Approach of Molecularly Imprinted Polymer,» vol. 7, n. 5, pp. 155-178, 2006. doi:10.3390/i7050155

[33] M. J. R. M. E. V. P. V. E. N. Whitcombe, «A New Method for the Introduction of Recognition Site Functionality into Polymers Prepared by Molecular Imprinting: Synthesis and Characterization of Polymeric Receptors for Cholesterol,» *Journal of the American Chemical Society,* 1995. doi:10.1021/ja00132a010

[34] K. J. S. Börje Sellergren, «Influence of polymer morphology on the ability of imprinted network polymers to resolve enantiomers,» *Journal of Chromatography A,* vol. 635, n. 1, pp. 31-49, 1993. doi:10.1016/0021-9673(93)83112-6

[35] J. W. L. W. Y. L. J. J. F. S. Y. T. J. C. Peipei Qi, «Molecularly imprinted polymers synthesized via semi-covalent imprinting with sacrificial spacer for imprinting phenols,» vol. 51, n. 23, 2010. doi:10.1016/j.polymer.2010.09.037

[36] G. A. O. Jennifer E. Lofgreen, «Controlling morphology and porosity to improve performance of molecularly imprinted sol–gel silica,» *Chemical Society Reviews,* n. 3, 2014. doi:10.1039/C3CS60276A

[37] J. J. G.-G. A. A. J. M. P.-S. L. C.-A. Abderrahman Lamaoui, «Chapter 4 - Synthesis techniques of molecularly imprinted polymer composites,» *Molecularly Imprinted Polymer Composites,* pp. 49-91, 2021. doi:10.1016/B978-0-12-819952-7.00002-0

[38] L. &. C. P. &. C. M. &. S. K. &. L. M. &. L. A. &. C. R. &. D. G. Piscopo, «Uniformly sized molecularly imprinted polymers (MIPs) for 17β-estradiol,» *Macromolecular Chemistry and Physics,* 2002. doi:10.1002/1521-3935(200207)203:10/11<1532::AID-MACP1532>3.0.CO;2-C

[39] A. A. B. M. G. Udduttula, «Molecularly Imprinted Polymers: Shaping the Future of Early-Stage Bone Loss Detection–A Review,» vol. 9, n. 8, 2024. doi:10.1021/acsomega.3c08977

[40] L. Z. Y. X. a. Y. Z. X. He, «An overview of photopolymerization and its diverse applications,» vol. 2, n. 6, 2023. doi:10.1002/appl.202300030

[41] J. S. R. C. N. D. N. Saleh Alghamdi S, «Additive Manufacturing of Polymer Materials: Progress, Promise and Challenges,» 2021. doi:10.3390/polym13050753

[42] W. X. M. S. Layani M, «Novel Materials for 3D Printing by Photopolymerization,» 2018. doi:10.1002/adma.201706344

[43] K. L. Sampson, B. Deore, A. Go, M. A. Nayak, A. Orth, M. Gallerneault, P. R. L. Malenfant e C. Paquet, «Multimaterial Vat Polymerization Additive Manufacturing,» vol. 3, n. 9, 2021. doi:10.1021/acsapm.1c00262

[44] P. M. L. G. M. D. A. Rezanavz R., «Three-Dimensional Printing of Molecularly Imprinted Polymers by Digital Light Processing for Copper Ion Sequestration,» 2022. doi:10.1089/3dp.2022.0107

[45] L. S. A. T. X.-A. F. Y. B. F. M. J.-P. T. S. B. B. T. D. A. C. H. K. a. S. O. Gomez, «Rapid Prototyping of Chemical Microsensors Based on Molecularly Imprinted Polymers Synthesized by Two-Photon Stereolithography,» vol. 28, n. 28, 2016. doi:10.1002/adma.201600218

[46] P. I. N. P. A. D. S. B. W. D. F. N. Z. X. R. M. a. S. K. Conrad, «Functional Molecularly Imprinted Polymer Microstructures Fabricated Using Microstereolithography,» pp. 1541-1544, 2003. doi:10.1002/adma.200304602

[47] W. S. B. Z. H. H. L. Z. Xing R, «Preparation of molecularly imprinted polymers specific to glycoproteins, glycans and monosaccharides via boronate affinity controllable-oriented surface imprinting.,» pp. 964-987, 2017. doi:10.1038/nprot.2017.015

[48] L. J.-M. L. C.-G. P. S.-J. J. E.-H. Lee Youn-Jun, «Photodegradation Behavior of Agricultural Antibiotic Oxytetracycline in Water,» vol. 14, n. 21, p. 3379, 2022. doi:10.3390/w14213379

[49] S. Y. D. M. A. M. B. G. Amangelsin Y, «The Impact of Tetracycline Pollution on the Aquatic Environment and Removal Strategies.,» *Antibiotics (Basel),* vol. 12, n. 3, 2023. doi:10.3390/antibiotics12030440

[50] H. E. D. B. &. D. B. KARA, «Highly luminescent water-dispersed silicon quantum dots for fluorometric determination of oxytetracycline in milk samples,» *Turkish Journal of Chemistry,* vol. 44, n. 6, pp. 1713-1722, 2020. doi:10.3906/kim-2007-4

[51] Sigma aldrich- OTC, [Online]. Available: https://www.sigmaaldrich.com/IT/it/substance/oxytetracycline4604379572. [Accessed 13 July 2025].

[52] G. L. M. H. Wang X, «Analysis of local polarity change around Cys34 in bovine serum albumin during N-->B transition by a polarity-sensitive fluorescence probe,» *Spectrochim Acta A Mol Biomol Spectrosc.,* vol. 73, n. 5, pp. 875-8, 2009. doi:10.1016/j.saa.2009.04.008

[53] M. P. D. P. M. P. S. L. B. R. B. A. P. B. Behera S, «Selective Binding of Bovine Serum Albumin (BSA): A Comprehensive Review,» *Biointerface Research in Applied Chemistry,* vol. 13, n. 6, 2023. doi:10.33263/BRIAC136.555

[54] W. P. W. C. K. L. Brandes N, «Adsorption-induced conformational changes of proteins onto ceramic particles: differential scanning calorimetry and FTIR analysis,» vol. 299, n. 1, pp. 56-69, 2006. doi:10.1016/j.jcis.2006.01.065

[55] T.-C. C. Chih-Hsien Hu, «Albumin molecularly imprinted polymer with high template affinity — Prepared by systematic optimization in mixed organic/aqueous media,» *Microchemical Journal,* vol. 91, n. 1, pp. 53-58, 2009. doi:10.1016/j.microc.2008.07.005

[56] R. J. G.-B. F. G.-R. J. S.-C. S. Sevilla P, «Identification of the antitumoral drug emodin binding sites in bovine serum albumin by spectroscopic methods,» *Biochim Biophys Acta,* vol. 1774, n. 11, pp. 1359-69, 2007. doi:10.1016/j.bbapap.2007.07.022

[57] S. Z. Hu T, «A solid phase adsorption method for preparation of bovine serum albumin-bovine hemoglobin conjugate,» *J Biotechnol,* vol. 100, n. 3, pp. 267-75, 2003. doi:10.1016/s0168-1656(02)00246-8

[58] L. J. L. X. G. B. C. J. S. Y. Wang Y, «Spectroscopic and molecular docking studies on binding interactions of camptothecin drugs with bovine serum albumin,» vol. 15, n. 1, 2025. doi:10.1038/s41598-025-92607-3

[59] Aozeal, [Online]. Available: https://www.aozeal.com/product/M0083.00/. [Accessed 13 July 2025].

[60] «Chemical Book,» [Online]. Available: https://www.chemicalbook.com/ChemicalProductProperty_EN_CB1494912.htm. [Accessed 13 July 2025].

[61] https://www.sigmaaldrich.com/IT/it/product/aldrich/282731?srsltid=AfmBOopqhqBokHgNL63o2gGnEb4idORDuEsr9zLj7m8qXmZ3hhhy-gxr, «Sigma aldrich- AMPS,» [Online]. [Accessed 13 July 2025].

[62] «Sigma Aldrich-HEMA,» [Online]. Available: https://www.sigmaaldrich.com/IT/it/product/aldrich/477028. [Accessed 13 July 2025].

[63] «Sigma Aldrich-NIPAM,» [Online]. Available: https://www.sigmaaldrich.com/IT/it/product/aldrich/252875. [Accessed 13 July 2025].

[64] Allnex- DPDGA, [Online]. Available: https://allnex.com/en/product/82a3a083-2bdd-46a5-abcc-11eb48f59dfd/dpgda.

[65] V. B. F. F. M. C. S. L. M. I. R. Elena Camilli, «Digital light processing 3D printing of molecularly imprinted polymers for antibiotic removal,» *Reactive and Functional Polymers,* vol. 208, 2025.

[66] Fisher - DPDGA, [Online]. Available: https://www.fishersci.ca/shop/products/dipropylene-glycol-diacrylate-stabilized-mehq-tci-america-3/p-7127745. [Accessed 13 July 2025].

[67] Polysciences- PEGDA, [Online]. Available: https://polysciences.com/products/polyethylene-glycol-n-diacrylate. [Accessed 13 July 2025].

[68] Sigma Aldrich- PEGDA. [Online]. [Accessed 13 July 2025].

[69] ACS-DMSO. [Online]. [Accessed 13 July 2025].

[70] Gaylord chemical-DMSO, [Online]. Available: https://www.gaylordchemical.com/products/literature/physical-properties/. [Accessed 13 July 2025].

[71] «Sigma Aldrich-DMSO,» [Online]. Available: https://www.sigmaaldrich.com/IT/it/product/sigma/d8418?srsltid=AfmBOoo7IUT-rCoKULMjGOO3_GFP1IMbqCPdGhfs0llPn_0TEa1V3QdP.

[72] Chimica-online H2O, [Online]. Available: https://www.chimica-online.it/download/molecola-dell-acqua.htm. [Accessed 13 July 2025].

[73] Benchchem, [Online]. Available: https://www.benchchem.com/product/b061975. [Accessed 13 July 2025].

[74] ReAgent- methyl red, [Online]. Available: https://www.chemicals.co.uk/blog/what-is-methyl-red?srsltid=AfmBOopfiKAeCpC1AJE8ylPpxWe1vDwjjgmjVkabo9nCFreUgxo0OnI3. [Accessed 13 July 2025].

[75] Sigma Aldrich - methyl red, [Online]. Available: https://www.sigmaaldrich.com/IT/it/product/sial/08714?utm_source=google&utm_medium=cpc&utm_campaign=21609945775&utm_content=173112201024&gad_source=1&gad_campaignid=21609945775&gbraid=0AAAAD8kLQSzQp7jplQc9xNmUYjDKuBXg&gclid=CjwKCAjw7MLDBhAuEiwAIeXGIRoXca.

[76] Reologia, [Online]. Available: https://wiki.anton-paar.com/it-it/fondamenti-della-reologia/. [Accessed 13 July 2025].

[77] B.W. Darvell, «Chapter 10 - Surfaces,» in *Materials Science for Dentistry*, Woodhead Publishing, 2018, pp. 292--336. doi:10.1016/B978-0-08-101035-8.50010-9

[78] UV-Vis, [Online]. Available: https://www.technologynetworks.com/analysis/articles/uv-vis-spectroscopy-principle-strengths-and-limitations-and-applications-349865. [Accessed 13 July 2025].

[79] M. Penner, «Basic Principles of Spectroscopy,» in *Nielsen, S.S. (eds) Food Analysis*, Springer, Cham, 2017. doi:10.1007/978-3-319-45776-5_6

[80] C. F. Z. M. V. G. B. C. B. S. M. S. F. A. R. I. Gastaldi M., «Functional Dyes in Polymeric 3D Printing: Applications and Perspectives,» vol. 3, n. 1, 2021. doi:10.1021/acsmaterialslett.0c00455

[81] N.C J. X. W. Y Ran D.«Bovine serum albumin recognition via thermosensitive molecular imprinted macroporous hydrogels prepared at two different temperatures,» pp. 45-53, 2012. doi:10.1016/j.aca.2012.02.020

[82] Z. T. K. M. Y. e. a. Shen, «Synthesis and phase behavior of aqueous poly(N-isopropylacrylamide-co-acrylamide), poly(N-isopropylacrylamide-co-N,N-dimethylacrylamide) and poly(N-isopropylacrylamide-co-2-hydroxyethyl methacrylate).,» *Colloid Polym Sci,* 2006. doi:10.1007/s00396-005-1442-y

[83] «https://nexa3d.com/blog/3d-printing/,» [Online]. [Accessed 13 July 2025].

[84] C. Michele, Studio della bagnabilità di superfici strutturate con nanofibre, 2013/2014.